

Adaptive Stereographic MCMC

Cameron Bell, Krzysztof Łatuszyński and Gareth O. Roberts

Department of Statistics, University of Warwick, United Kingdom

August 2024

Abstract

In order to tackle the problem of sampling from heavy tailed, high dimensional distributions via Markov Chain Monte Carlo (MCMC) methods, Yang, Łatuszyński, and Roberts 2022 introduces the stereographic projection as a tool to compactify \mathbb{R}^d and transform the problem into sampling from a density on the unit sphere \mathbb{S}^d . However, the improvement in algorithmic efficiency, as well as the computational cost of the implementation, are still significantly impacted by the parameters used in this transformation.

To address this, we introduce adaptive versions of the Stereographic Random Walk (SRW), the Stereographic Slice Sampler (SSS), and the Stereographic Bouncy Particle Sampler (SBPS), which automatically update the parameters of the algorithms as the run progresses. The adaptive setup allows us to better exploit the power of the stereographic projection, even when the target distribution is neither centered nor homogeneous. We present a simulation study showing each algorithm's robustness to starting far from the mean in heavy tailed, high dimensional settings, as opposed to Hamiltonian Monte Carlo (HMC). We establish a novel framework for proving convergence of adaptive MCMC algorithms over collections of simultaneously uniformly ergodic Markov operators, including continuous time processes. This framework allows us to prove LLNs and a CLT for our adaptive Stereographic algorithms.

1 Introduction

Markov Chain Monte Carlo (MCMC) algorithms are used to approximate a given target distribution π on \mathbb{R}^d , typically arising in the context of Bayesian inference. For this purpose, a Markov process is simulated which admits π as its stationary

distribution, and we can use its empirical distribution to approximate π . It is therefore crucial for our algorithms to quickly converge to stationarity, and efficiently explore the entire target distribution. We will be primarily discussing the case where π is unimodal, and refer to the many other works attempting to address the challenges of sampling from multimodal targets (e.g. Tawn, Moores, and Roberts 2021; Pompe, Holmes, and Łatuszyński 2020).

From the Random Walk Metropolis algorithm (RWM) (Metropolis et al. 1953; Hastings 1970) to Hamiltonian Monte Carlo (HMC) (Neal 2012), many MCMC algorithms rely on local moves to explore the space. Even more sophisticated algorithms such as the Zig-Zag algorithm (Bierkens, Fearnhead, and Roberts 2019) or the Bouncy Particle Sampler (BPS) (Bouchard-Côté, Vollmer, and Doucet 2018) only move at a fixed speed, although versions of these algorithms exist with non-constant speeds (Bierkens, Grazi, et al. 2020; Vasdekis and Roberts 2023). If π is heavy tailed, a large amount of probability mass will be spread far from the mode of the target. All the above algorithms will struggle to efficiently mix when targeting such distributions because they have a tendency to get lost out in one corner of the tails, follow near-Brownian dynamics, and take an eternity to return to the mode. These problems are only made worse by the “curse of dimensionality”: as the dimension d increases, more and more of the volume in \mathbb{R}^d is away from the mode, so there is “more” tail that needs efficiently exploring, whilst still needing to return quickly to the center of the target.

A common way of assessing convergence of Markov processes is via a geometric ergodicity result, such as:

$$\|P^t(x, \cdot) - \pi\|_{\text{TV}} \leq C(x)\rho^t, \quad (1.1)$$

for π -almost every $x \in \mathbb{R}^d$, t either in \mathbb{N} or $[0, \infty)$ depending on the context, and $\rho < 1$. If an MCMC algorithm is geometrically ergodic, the chain has good mixing properties such as the existence of a Central Limit Theorem (CLT) (Meyn and Tweedie 2012), and we expect it to converge quickly to its stationary distribution.

Deligiannidis, Bouchard-Côté, and Doucet 2019, Table 1 summarises results on whether various algorithms are geometrically ergodic depending on the tail behaviour of the target. Indeed, without including any transformations of the target distribution, standard algorithms struggle to sample from heavy tailed distributions and only exhibit polynomial convergence to stationarity.

If $C(x) \leq C$ is uniformly bounded over x , we say that the Markov process is uniformly ergodic. In this case, we expect the chain to quickly return to the modal region from the tails of the target, regardless of how far out we are, leading to even better mixing properties. However, it can be shown that the algorithms discussed above are typically only uniformly ergodic when π is bounded and has a compact support (see Mengersen and Tweedie 1996 for the discussion in the case of RWM).

With this motivation, it is natural to attempt to transform the sample space onto a compact set, then sample from the transformed target distribution on the new support. Yang, Latuszyński, and Roberts 2022 achieve this via the stereographic projection: this map transforms Euclidean space \mathbb{R}^d onto \mathbb{S}^d/N , the unit sphere with the North pole $N = (0, \dots, 0, 1)$ removed. In this setting, N can be seen as the “image of ∞ ” under the map. Although this image is not compact, it is bounded and allows algorithms to reach anywhere in the state space a bounded time using only local moves on \mathbb{S}^d . Their algorithms are shown to be uniformly ergodic for a wide range of target distributions, including heavy tailed targets, and even exhibit a “blessing of dimensionality” in ideal settings, converging to stationarity faster as d increases.

However, uniform ergodicity alone does not immediately translate to incredible sampling properties. If the target distribution π is poorly preconditioned, the probability mass will be concentrated on a very small part of the sphere, which locally looks to our algorithms like a very small version of \mathbb{R}^d . We therefore parametrise the stereographic projection in order to attempt to evenly distribute the probability mass around \mathbb{S}^d . This is equivalent to preconditioning π to be centered and appropriately scaled.

With optimally chosen parameters, the probability mass becomes concentrated and uniformly spread around the equator of the sphere. In practice, however, we will not know the optimal values for these parameters before running the algorithm. A natural way of addressing this challenge is therefore to automatically update the parameters based on the history of the chain, and use these new, hopefully improved parameters in future transitions. This framework is known as adaptive MCMC, and is a relatively well studied area (Roberts and Rosenthal 2007; Roberts and Rosenthal 2009).

To address the issues of potentially poorly specified parameters in the stereographic algorithms, in this paper we create adaptive frameworks to update the parameters as we run our processes:

- we present adaptive versions of the 3 stereographic MCMC algorithms we discuss;
- we demonstrate each algorithm’s ability to tune the parameters according to the target distribution via a toy example;
- we provide a unifying theorem giving appropriate conditions for Weak or Strong Laws of Large Numbers (LLN) and a CLT in each case;
- we prove this by showing that such a theorem holds when creating an adaptive version of any uniformly ergodic Markov process.

In Section 2, we formally introduce the stereographic projection, then the three algorithms: the Stereographic Random Walk (SRW), the Stereographic Slice Sampler (SSS) and the Stereographic Bouncy Particle Sampler (SBPS). The SRW and SBPS were first presented in Yang, Łatuszyński, and Roberts 2022, and the SSS is presented in Habeck et al. 2023 under the name geodesic slice sampler.

In Section 3, we present our adaptive versions of each of the algorithms. Our algorithms are based on the Adapting Increasingly Rarely (AIR) MCMC setup from Chimisov, Łatuszyński, and Roberts 2018. We present a toy example demonstrating the ability of our algorithms to adapt the parameters of the transformation. These simulations clearly demonstrate the stereographic algorithms’ ability to start deep in the tails of heavy tailed, high dimensional target distributions with poor initial parameter choices and still find the modal region. By comparison, HMC fails to make any progress on finding the mode.

We state the main convergence results in Theorem 3.5. To theoretically justify the application of the AIR MCMC framework to our setting, in Section 4, we create a novel auxiliary process, which we dub the segment chain. We show a Law of Large Numbers (LLN) and a CLT for the segment chain, and show that any uniformly ergodic Markov process, whether discrete or continuous time, inherits these results.

2 Stereographic MCMC

We start by defining the stereographic projection, then the three algorithms: the Stereographic Random Walk (SRW), the Stereographic Slice Sampler (SSS) and the Stereographic Bouncy Particle Sampler (SBPS).

2.1 The Stereographic Projection

The stereographic projection is a diffeomorphism from the punctured unit sphere $\mathbb{S}^d/\{N\}$, where $N = (0, \dots, 0, 1)$ is the “North pole”, to \mathbb{R}^d . Figure 1 presents the geometric intuition of the stereographic projection in the case $d = 1$.

Generalising to higher dimensions, given a vector $\mu \in \mathbb{R}^d$ and a positive definite matrix $\Sigma \in \mathbb{R}^{d \times d}$, the (preconditioned) stereographic projection of a point $z \in \mathbb{S}^d$ gives:

$$x = \Sigma^{1/2} \left(\frac{z_1}{1 - z_{d+1}}, \dots, \frac{z_d}{1 - z_{d+1}} \right) + \mu, \quad (2.1)$$

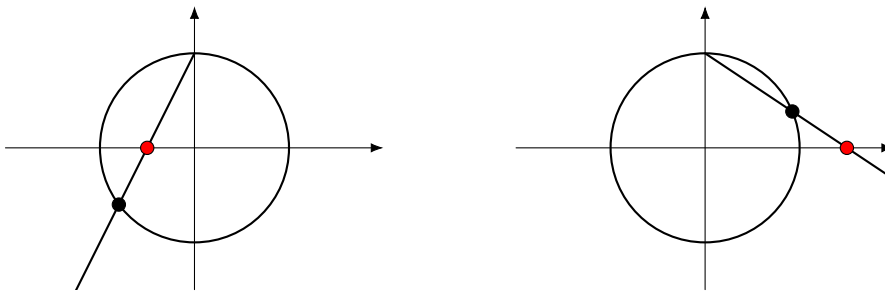


Figure 1: The stereographic projection from \mathbb{R} to \mathbb{S}^1 : given $x \in \mathbb{R}$, we draw a line between x (red) and the North pole $N = (0, 1)$, and define the projected point $z \in \mathbb{S}^1$ (black) to be point where the ray intersects the circle. We see that as $x \rightarrow \pm\infty$, $z \rightarrow N$.

and:

$$\begin{aligned} z_{1:d} &= \frac{2\Sigma^{-1/2}(x - \mu)}{\|\Sigma^{-1/2}(x - \mu)\|^2 + 1}, \\ z_{d+1} &= \frac{\|\Sigma^{-1/2}(x - \mu)\|^2 - 1}{\|\Sigma^{-1/2}(x - \mu)\|^2 + 1}. \end{aligned} \tag{2.2}$$

This can be thought of as projecting from z to $\tilde{x} = \frac{z_{1:d}}{1 - z_{d+1}}$, then preconditioning to obtain $x = \Sigma^{1/2}\tilde{x} + \mu$.

Setting $\gamma = (\mu, \Sigma)$ to be the parameter of the transformation, let Γ be the full parameter space. We write $x = \text{SP}_\gamma(z)$ and $z = \text{SP}_\gamma^{-1}(x)$ for the stereographic projection map and its inverse.

N can be thought of as the image of ∞ under the stereographic projection because as $z \rightarrow N$, $\|\text{SP}_\gamma(z)\| \rightarrow \infty$. Moreover, we can travel vast distances in \mathbb{R}^d by taking a very small step within the vicinity of the North Pole in \mathbb{S}^d . This will allow our MCMC algorithms to quickly explore the tails of the target distribution, then return to the high probability region.

This contraction of space is also clear from the Jacobian of the transformation, which is $\frac{\partial z}{\partial x} \propto |\Sigma^{1/2}|^{-1}(1 + \|\Sigma^{-1/2}(x - \mu)\|^2)^d$. As $\|\Sigma^{-1/2}(x - \mu)\|$ increases, so does the shrinkage of space provided by the stereographic projection.

The target density $\pi(x)$ on \mathbb{R}^d is then transformed to the following distribution on \mathbb{S}^d :

$$\begin{aligned} \pi_\gamma(z) &\propto |\Sigma^{1/2}|^{-1} \pi(x) (1 + \|\Sigma^{-1/2}(x - \mu)\|^2)^d \\ &\propto |\Sigma|^{-1/2} \pi(x) (1 - z_{d+1})^{-d}, \end{aligned} \tag{2.3}$$

where the proportionality is independent of γ . For example, for $\pi(x) \propto (d + \|x\|^2)^d$ a multivariate t -distribution with $\nu = d$ degrees of freedom, then π_γ is uniform on \mathbb{S}^d when $\mu = 0_d$ and $\Sigma = dI_d$.

2.2 Markov Processes on the Sphere

Given the transformed density π_γ on \mathbb{S}^d , we now discuss algorithms to efficiently sample from densities on the unit sphere.

2.2.1 The Stereographic Random Walk

We start with the SRW, a random walk Metropolis algorithm on the sphere. This algorithm is the first one presented in Yang, Łatuszyński, and Roberts 2022 under the name stereographic projection sampler. We rename it as SRW to more easily distinguish between the acronyms. Given a position $z \in \mathbb{S}^d$, we propose the next point by taking a Gaussian step in the hyperplane tangent to \mathbb{S}^d at z , then normalising the vector to return to \mathbb{S}^d . This proposal scheme is shown in Figure 2.

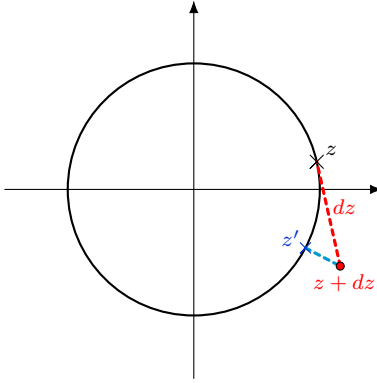


Figure 2: An SRW proposal

To implement this, from a position z , we sample $\tilde{d}z \sim \mathcal{N}(0, h^2 I_{d+1})$ and set $dz = \tilde{d}z - (z \cdot \tilde{d}z)z$ to be the Gaussian step orthogonal to z . We then let our proposal point be $z' = \frac{z + dz}{\|z + dz\|}$. The symmetrical nature of the Gaussian distribution ensures the proposal kernel $q(z, z')$ is reversible with respect to the uniform measure on \mathbb{S}^d :

$$q(z, z') = q(z', z). \quad (2.4)$$

We then accept z' as the new position by applying the Metropolis ratio to π_γ . The overall algorithm is given in Algorithm 1.

From Equation (2.4), this is a random walk Metropolis algorithm and has invariant measure π_γ on \mathbb{S}^d .

Algorithm 1 The Stereographic Random Walk

Input: Target density π on \mathbb{R}^d , $X_0 \in \mathbb{R}^d$, parameters $\gamma \in \Gamma$, $h > 0$, $Z_0 = \text{SP}_\gamma^{-1}(X_0)$

Output: $\{(X_n, Z_n)\}_{n \in \mathbb{N}}$

For $n = 0, 1, \dots$:

- Sample $\tilde{d}z \sim \mathcal{N}(0, h^2 I_{d+1})$ in \mathbb{R}^{d+1} , and set $dz = \tilde{d}z - (\tilde{d}z \cdot Z_n)Z_n$
- Set $z' = \frac{Z_n + dz}{\|Z_n + dz\|}$, and set $Z_{n+1} = z'$ with probability:

$$\min\left(\frac{\pi_\gamma(z')}{\pi_\gamma(Z_n)}, 1\right) = \min\left(\frac{\pi(x')(1 - z'_{d+1})^{-d}}{\pi(X_n)(1 - Z_{n,d+1})^{-d}}, 1\right),$$

where $x' = \text{SP}_\gamma(z')$. Otherwise, set $Z_{n+1} = Z_n$

- Set $X_{n+1} = \text{SP}_\gamma(Z_{n+1})$
-

2.2.2 The Stereographic Slice Sampler

Habeck et al. 2023 present the geodesic slice sampler as a method for sampling from distributions on \mathbb{S}^d . We repurpose it as the SSS and apply it to π_γ .

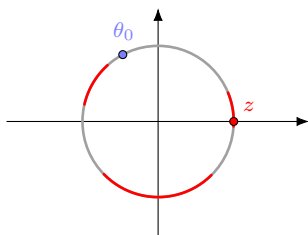
From a position $z \in \mathbb{S}^d$, we start by sampling v uniformly from the set $\{z\}^\perp = \{v \in \mathbb{S}^d : v \cdot z = 0\}$, i.e. $v \sim p(\cdot|z)$ where:

$$p(dv|z) = \frac{dv}{|\mathbb{S}^{d-1}|} \mathbb{1}(v \cdot z = 0), \quad (2.5)$$

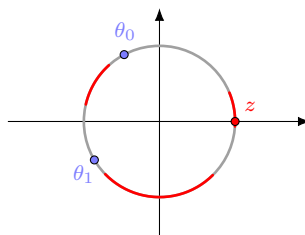
to define a geodesic of the form $z \cos(\theta) + v \sin(\theta)$ for $\theta \in [0; 2\pi)$. We then aim to perform a slice sampling step targeting the measure on the one dimensional geodesic with density π_γ . We start by sampling $t \sim U(0, \pi_\gamma(z))$, then wish to sample a new position z' uniformly from the superlevel set:

$$L_{z,v}(t) = \{z' = z \cos(\theta) + v \sin(\theta) : \theta \in [0, 2\pi), \pi_\gamma(z') > t\}. \quad (2.6)$$

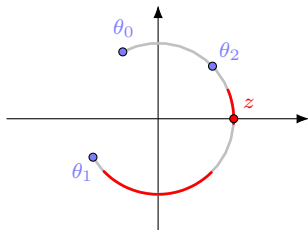
Working on a fixed geodesic, this slice sampler can be thought of as a Gibbs sampler targeting the joint distribution on (z, t) with density proportional to $\mathbb{1}(\pi_\gamma(z) > t)$. In practice, exact sampling from the uniform distribution on $L_{z,v}(t)$ requires rejection sampling and can be very inefficient. Habeck et al. 2023 therefore implements this step as a Metropolis-within-Gibbs step using adaptive rejection sampling, referred to as the shrinkage procedure. This process is depicted geometrically in Figure 3, and explicitly stated in Algorithm 2.



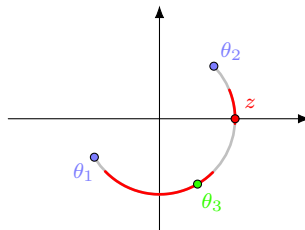
(a) We start with an initial proposal θ_0 .



(b) If we reject θ_0 , propose a new point.



(c) If we reject θ_1 , remove the segment which does not contain z . Sample θ_2 uniformly from the new interval.



(d) Repeat this process, iteratively shrinking the size of the interval around z , until we propose a point in $L_{z,v}(t)$.

Figure 3: The Shrinkage Procedure for the Stereographic Slice Sampler: consider the set $L_{z,v}(t)$ in red, and sequentially shrink the interval of interest by using the rejected points.

The shrinkage procedure, which we denote $\text{Shrink}(z, v, t)$ is then incorporated into a full Markov kernel: given a current position $Z_n = z \in \mathbb{S}^d$, we sample $t \sim U(0, \pi_\gamma(z))$, $v \sim p(\cdot|z)$, then sample $Z_{n+1} \sim \text{Shrink}(z, v, t)$. We summarise this in Algorithm 3. Habeck et al. 2023 proves in Lemma 24 that this Markov kernel is π_γ reversible, and therefore has the correct stationary distribution.

2.2.3 The Stereographic Bouncy Particle Sampler

Our last algorithm, the SBPS, is the second algorithm presented in Yang, Łatuszyński, and Roberts 2022, and is a Piecewise Deterministic Markov Process (PDMP) targeting π_γ . Unlike the previous two algorithms, it is defined as a continuous time process over:

$$\mathbb{S}^d \perp \mathbb{S}^d = \{(z, v) \in \mathbb{S}^d \times \mathbb{S}^d : z \cdot v = 0\}, \quad (2.7)$$

where the position z is considered to be our sample point, and the velocity v is a latent variable used to explore the space. Given an initial pair $(z_0, v_0) \in \mathbb{S}^d \perp \mathbb{S}^d$, the process evolves deterministically along a geodesic, according to the dynamics:

$$\begin{aligned} z(t) &= z_0 \cos(t) + v_0 \sin(t), \\ v(t) &= v_0 \cos(t) - z_0 \sin(t). \end{aligned} \quad (2.8)$$

Algorithm 2 The Shrinkage Procedure for the Stereographic Slice Sampler

Input: Target density p on \mathbb{S}^d , orthogonal pair $(z, v) \in \mathbb{S}^d \perp \mathbb{S}^d$, level $t \in (0, p(z))$

Output: $z' \in L_{z,v}(t)$

Initialisation: Sample $\theta \sim U(0, 2\pi)$, and set $\theta_{\max} = \theta$, $\theta_{\min} = \theta - 2\pi$

While $p(z \cos(\theta) + v \sin(\theta)) \leq t$:

- **If** $\theta < 0$: Set $\theta_{\min} = \theta$
- **Else:** Set $\theta_{\max} = \theta$
- Resample $\theta \sim U(\theta_{\min}, \theta_{\max})$

Return: $z' = z \cos(\theta) + v \sin(\theta)$.

Algorithm 3 The Stereographic Slice Sampler

Input: Target density π on \mathbb{R}^d , $X_0 \in \mathbb{R}^d$, parameter $\gamma \in \Gamma$, $Z_0 = \text{SP}_\gamma^{-1}(X_0)$

Output: $\{(X_n, Z_n)\}_{n \in \mathbb{N}}$

For $n = 0, 1, \dots$:

- Sample $T_n \sim U(0, \pi_\gamma(Z_n))$, and $V_n \sim p(\cdot | Z_n)$
 - Sample $Z_{n+1} \sim \text{Shrink}(Z_n, V_n, T_n)$ according to the shrinkage procedure in Algorithm 2
 - Set $X_{n+1} = \text{SP}_\gamma(Z_{n+1})$
-

We then introduce two types of random events at which we change the velocity v . Bounce events occur according to an inhomogeneous Poisson process with rate $\chi(t) = \lambda(z(t), v(t))$, where:

$$\lambda(z, v) = \max \left[0, -v \cdot \nabla_z \log \pi_\gamma(z) \right]. \quad (2.9)$$

Note that bounce events cannot happen if $\log \pi_\gamma(z(t))$ is increasing, and otherwise is equal to $-\frac{d \log \pi_\gamma(z(t))}{dt}$.

Refreshment events occur according to a homogeneous Poisson process with constant rate $\lambda_{\text{ref}} > 0$ independently of the current state of the process. This gives a total event rate of:

$$\bar{\lambda}(z, v) = \lambda(z, v) + \lambda_{\text{ref}}, \quad (2.10)$$

when the process is at (z, v) . Conditionally on an event occurring at (z, v) , it is a refreshment event with probability $\lambda_{\text{ref}} / \bar{\lambda}(z, v)$.

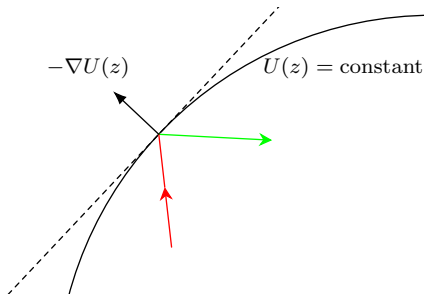


Figure 4: Illustration of a Bounce Event. Here, the target density is taken to be of the form $\pi_\gamma(z) \propto \exp(U(z))$ for some function $U(z)$. The particle initially travels “downhill” along the red path before bouncing at a specific time. At the event time, the particle lies on the black contour of $U(z)$ and “bounces” away from it

Once an event occurs, we resume our deterministic dynamics according to Equation (2.8), but with the new velocity.

For a bounce event at (z, v) , we update the velocity v by reflecting its component in the direction of the gradient of $\log \pi_\gamma$ to:

$$v' = v - 2 \frac{v \cdot \tilde{\nabla}_z \log \pi_\gamma(z)}{\|\tilde{\nabla}_z \log \pi_\gamma(z)\|^2} \tilde{\nabla}_z \log \pi_\gamma(z), \quad (2.11)$$

where the $\tilde{\nabla}_z$ operator refers to the gradient tangent to the sphere at z , and is expressed by:

$$\tilde{\nabla}_z U(z) = \nabla_z U(z) - (z \cdot \nabla_z U(z))z, \quad (2.12)$$

for an arbitrary function U . Geometrically, the path of the particle around bounce events is described in Figure 4.

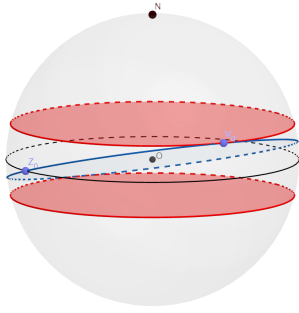
We let $R(z)$ be the matrix:

$$R(z) = I_{d+1} - 2 \frac{\tilde{\nabla}_z \log \pi_\gamma(z) \tilde{\nabla}_z \log \pi_\gamma(z)^T}{\|\tilde{\nabla}_z \log \pi_\gamma(z)\|^2}, \quad (2.13)$$

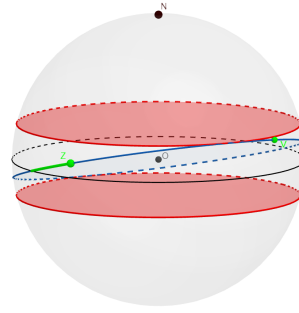
so that $v' = R(z)v$ for a bounce event at (z, v) .

At the independent refreshments, we sample $v' \sim p(\cdot|z)$ uniformly from $\{z\}^\perp$, as in Equation (2.5). As with the Euclidean BPS, including independent refreshments is necessary for irreducibility of the algorithm, as shown in Figure 5.

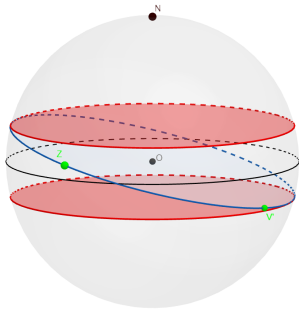
We denote (Z_t, V_t) the random position and velocity of the SBPS at time $t > 0$, and present the algorithm as a whole in Algorithm 4. Note that, computationally speaking, one will not be able to store or work with a continuous sample path. One can choose to either output a skeleton of the chain, sampled at regular time intervals of short length δ , or output the points at event times $\{(z^{(i)}, v^{(i)})\}_{i \in \mathbb{N}}$, although it is vital to note that these are not distributed according to π_γ .



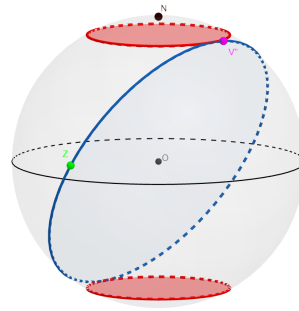
(a) Any SBPS path is constrained to a certain region around the equator.



(b) Running the dynamics keeps us there.



(c) Bounce events may not change these bounds on the latitude.



(d) Refreshment events allow the process to access the entire sample space.

Figure 5: SBPS Bounce Events do not allow the path to leave the vicinity of the equator when targeting a spherically symmetrical distribution, such as a $\mathcal{N}(0, I_d)$. Refreshment events are then required for irreducibility.

It is shown in Yang, Łatuszyński, and Roberts 2022 that the SBPS is ergodic, and its stationary distribution has density $\pi_\gamma(z) \times p(v|z)$ on $\mathbb{S}^d \perp \mathbb{S}^d$.

3 Adaptive Stereographic Algorithms

Each of the above algorithms is parametrised by γ , the parameters of the stereographic projection, and potentially additional parameters (h for the SRW and λ_{ref} for the SBPS). The choices of these parameters can heavily impact algorithmic performance. In this section, we establish motivation for optimal choices of γ and introduce our adaptive versions of each of the 3 algorithms.

Algorithm 4 The Stereographic Bouncy Particle Sampler

Input: Target density π_γ on \mathbb{S}^d , $(Z_0, V_0) \in \mathbb{S}^d \perp \mathbb{S}^d$, refreshment rate λ_{ref} .

Output: $\{(Z_t, V_t)\}_{t \in [0, \infty)}$.

Initialisation: Set $(z^{(0)}, v^{(0)}) = (Z_0, V_0)$ and $s = 0$.

For $i = 0, 1, \dots$:

- Sample $\tau_{\text{ref}} \sim \text{Exp}(\lambda_{\text{ref}})$
 - Sample τ_{bounce} according to the first event of a Poisson process with rate function $t \mapsto \lambda(z(t), v(t))$, with $(z(t), v(t))$ given by Equation (2.8) initialised at $(z^{(i)}, v^{(i)})$, and $\lambda(z, v)$ as in Equation (2.9)
 - Set $\tau = \min(\tau_{\text{ref}}, \tau_{\text{bounce}})$, and $Z(t+s) = z^{(i)} \cos(t) + v^{(i)} \sin(t)$, $V(t+s) = v^{(i)} \cos(t) - z^{(i)} \sin(t)$ for all $t \in [0, \tau)$
 - Set $s = s + \tau$ and $z^{(i+1)} = z^{(i)} \cos(\tau) + v^{(i)} \sin(\tau)$
 - **If** $\tau_{\text{ref}} < \tau_{\text{bounce}}$: sample $v^{(i+1)} \sim p(\cdot | z^{(i+1)})$
 - **Else:** set $v^{(i+1)} = R(z^{(i+1)})v^{(i)}$ as per Equation (2.13)
-

3.1 The Equator as a High Probability Region

We will be interested in varying γ in order to optimally position and scale the sphere to match properties of the target distribution π . Figure 6 shows that the choice of γ heavily impacts the behaviour of π_γ . Indeed, if $X_i \stackrel{\text{iid}}{\sim} f(x)$ with $\mathbb{E}_f(X_1) = 0$, $\mathbb{E}_f(X_1^2) = 1$, then taking $\gamma = (0, dI_d)$ gives:

$$Z_{d+1} = \frac{\frac{1}{d}\|X\|^2 - 1}{\frac{1}{d}\|X\|^2 + 1} = \mathcal{O}_{\mathbb{P}}(d^{-\frac{1}{2}}), \quad (3.1)$$

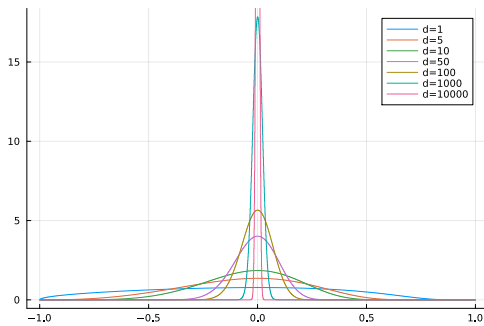
whereas if the eigenvalues of Σ are not of order d then π_γ will become concentrated around one of the poles.

We can therefore construct our algorithms to efficiently explore the equator, and tune our parameters to precondition the target by taking:

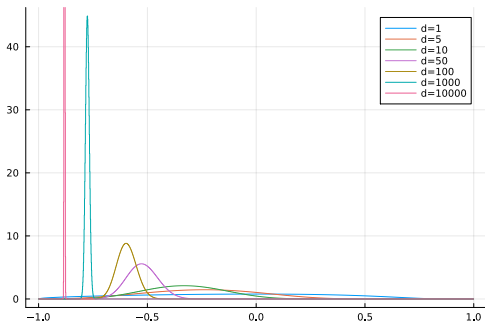
$$\mu = \mathbb{E}_\pi(X), \quad \Sigma = d \times \mathbb{E}_\pi((X - \mu)(X - \mu)^T). \quad (3.2)$$

Since we do not know these expectations in advance, it is of interest to create adaptive versions of any algorithm using the stereographic projection in order to automatically tune γ .

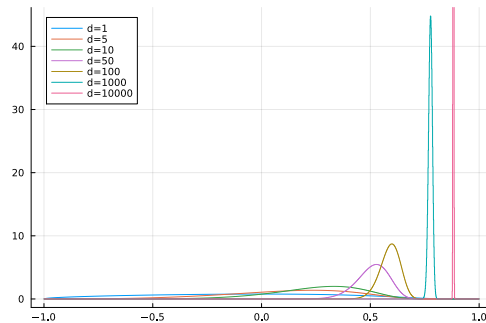
Each of our algorithms can be seen to have better mixing properties when γ is optimally chosen. For the SRW, Yang, Łatuszyński, and Roberts 2022 presents an



(a) Taking $\Sigma = dI_d$, we see that π_γ becomes concentrated around the equator $z_{d+1} = 0$.



(b) Taking $\Sigma = d^{1.3}I_d$, we see that the mass moves towards the South pole.



(c) Taking $\Sigma = d^{0.7}I_d$, we see that the mass moves towards the North pole.

Figure 6: Plots of the marginal density of Z_{d+1} under π_γ , when $X \sim \mathcal{N}(0, I_d)$. We fix $\mu = 0$ and vary Σ .

extensive discussion of this topic, proving that the algorithm can be superefficient in this setting. The geometry of \mathbb{S}^d causes proposed moves to naturally stay on the equator if that is where the chain lies, and drift back towards the equator if the chain is currently near either pole. Furthermore, these properties become stronger as d increases and the volume of the sphere also becomes concentrated on the equator, which is what produces the blessing of dimensionality.

We give sketch arguments in the case of the SSS or the SBPS. Both work from proposing moves along geodesics, which are more and more likely to represent a subset of the equator as d increases, and will always overlap with the equator regardless of the current position. Thus, the algorithms will naturally stay within the vicinity of the equator if that is where they are, and will attempt to return to the equator in $\mathcal{O}(1)$ time if the process is currently at one of the poles. Unlike the SRW, the SBPS and SSS also suffer computationally if π_γ is focused on a small

subset of \mathbb{S}^d : the SBPS will require many bounce events to fight the drift back towards the equator, and the rejection sampling step in the SSS will reject many moves at every step before narrowing down the search interval.

It is worth mentioning that adaptations can also be made for the other parameters, h and λ_{ref} . In the case of the SRW, Yang, Łatuszyński, and Roberts 2022 prove that if γ is chosen according to Equation (3.2), then in certain settings it is optimal to tune h such that we have an average acceptance rate of 0.234, as is the case for the Euclidean RWM algorithm (Gelman, Gilks, and Roberts 1997). The optimal refreshment rate for the SBPS is an open problem, but it is noteworthy that Bierkens, Kamatani, and Roberts 2022 shows that, for the Euclidean BPS, it is optimal in certain settings to have 78.1% of events be refreshment events.

3.2 The Algorithms

We now construct adaptive versions of the stereographic algorithms which automatically tune the parameters as they run, in order to improve performance. We established in Equation (3.2) what values we will be targeting with our estimators. However, as is the case for all adaptive MCMC algorithms, changing the transition scheme based on the past sample path so far causes the Markov property to fail.

There are plenty of frameworks for constructing discrete time adaptive MCMC algorithms with good asymptotic properties (Roberts and Rosenthal 2007; Roberts and Rosenthal 2009). On the other hand, we found no evidence in the literature of continuous time adaptive MCMC algorithms. In this paper, we use the Adapting Increasingly Rarely (AIR) MCMC framework from Chimisov, Łatuszyński, and Roberts 2018, and show that it can be applied to continuous time algorithms. Crucially, this makes the setup identical for each of our algorithms.

We assume the lags t_k between adaptations are polynomially increasing, i.e. that $\exists \beta > 0$ and $c \geq 1$ such that:

$$\frac{1}{c}k^\beta \leq t_k \leq ck^\beta, \quad (3.3)$$

and define the adaptation times $T_k = \sum_{i=1}^k t_i$. For consistency of notation, we take $T_0 = t_0 = 0$.

We proceed by running the process holding the parameter γ_k fixed for $t \in [T_k, T_{k+1})$. At each time T_{k+1} , we update the parameter to γ_{k+1} based on the sample path so far and the previous parameter values. The resulting algorithms are then given in Algorithms 5, 6, 7.

These AIR schemes have multiple benefits over the more commonly used adaptation schemes of adapting every step, or every k steps:

Algorithm 5 AIR SRW

Input: Target density π on \mathbb{R}^d , $X_0^{(0)} \in \mathbb{R}^d$, initial parameters $\gamma_0 \in \Gamma$, $h_0 > 0$, sequence of adaptation lags $\{t_k\}_{k \in \mathbb{N}}$.

Output: $\{(Z_n^{(k)}, X_n^{(k)})\}_{0 \leq n \leq t_k}$, γ_k and h_k , for $k \in \mathbb{N}$.

For $k = 0, 1, \dots$:

- Run the SRW (Algorithm 1) for t_{k+1} time units to get

$$\{(Z_n^{(k+1)}, X_n^{(k+1)})\}_{0 \leq n \leq t_{k+1}} \sim \text{SRW}(\pi, X_{t_k}^{(k)}, \gamma_k, h_k)$$

- Update parameters to γ_{k+1}, h_{k+1} using $\{(Z_n^{(k+1)}, X_n^{(k+1)})\}_{0 \leq n \leq t_{k+1}}$
-

Algorithm 6 AIR SSS

Input: Target density π on \mathbb{R}^d , $X_0^{(0)} \in \mathbb{R}^d$, initial parameters $\gamma_0 \in \Gamma$, sequence of adaptation lags $\{t_k\}_{k \in \mathbb{N}}$.

Output: $\{(Z_n^{(k)}, X_n^{(k)})\}_{0 \leq n \leq t_k}$ and γ_k , for $k \in \mathbb{N}$.

For $k = 0, 1, \dots$:

- Run the SSS (Algorithm 3) for t_{k+1} time units to get

$$\{(Z_n^{(k+1)}, X_n^{(k+1)})\}_{0 \leq n \leq t_{k+1}} \sim \text{SSS}(\pi, X_{t_k}^{(k)}, \gamma_k)$$

- Update parameters to γ_{k+1} using $\{(Z_n^{(k+1)}, X_n^{(k+1)})\}_{0 \leq n \leq t_{k+1}}$
-

- Practically speaking, at every adaptation, we will be trying to obtain an estimator for the square root of the covariance matrix to feed into our algorithms. Since there are no convenient iterative update schemes for this, we will need to recalculate a $d \times d$ covariance estimator and take its square root every time we adapt. In high dimensions, this can become very costly, so it is sensible to adapt more rarely as the process goes on and we expect the estimators to converge.
- Theoretically speaking, adaptive MCMC algorithms can be tricky to analyse because using the history of the chain to inform future transitions causes the Markov property to break down. By keeping the parameters fixed for increasing lengths of time, we obtain a sequence of epochs which conditionally behave like standard Markov chains, and these sample paths become easier

Algorithm 7 AIR SBPS

Input: Target density π on \mathbb{R}^d , $X_0^{(0)} \in \mathbb{R}^d$, initial parameters $\gamma_0 \in \Gamma$, $\lambda_0 > 0$, sequence of adaptation lags $\{t_k\}_{k \in \mathbb{N}}$.

Output: $\{(Z_t^{(k)}, V_t^{(k)}, X_t^{(k)})\}_{0 \leq t \leq t_k}$ and γ_k , for $k \in \mathbb{N}$.

For $k = 0, 1, \dots$:

- Set $z = \text{SP}_{\gamma_k}^{-1}(X_{t_k}^{(k)})$, and sample $v \sim p(\cdot|z)$
- Run the SBPS (Algorithm 4) for t_{k+1} time units to get

$$\{(Z_t^{(k+1)}, V_t^{(k+1)})\}_{0 \leq t \leq t_{k+1}} \sim \text{SBPS}(\pi_{\gamma_k}, (z, v), \lambda_k)$$

- Set $\{X_t^{(k+1)}\}_{0 \leq t \leq t_{k+1}} = \{\text{SP}_{\gamma_k}(Z_t^{(k+1)})\}_{0 \leq t \leq t_{k+1}}$
 - Update parameter to γ_{k+1} using $\{(Z_t^{(k+1)}, V_t^{(k+1)}, X_t^{(k+1)})\}_{0 \leq t \leq t_{k+1}}$
-

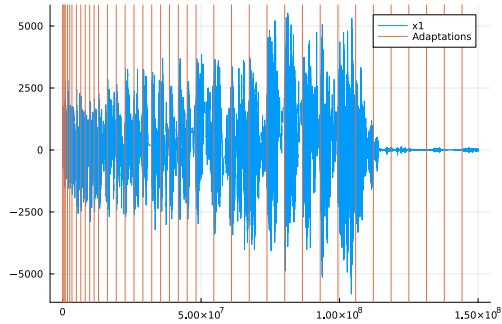
to control the longer they run for.

3.3 Simulation Studies

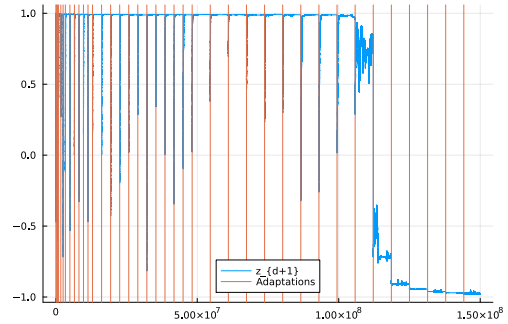
In Section 3.4, we will present our theoretical results with sufficient conditions to obtain LLNs or a CLT for our adaptive stereographic algorithms. First, however, we demonstrate the ability of our algorithms to optimise the parameters in heavy tailed, high dimensional settings.

Consider targeting a multivariate t -distribution with $\nu = 2$, $d = 200$, with initial parameters $\mu = (1000, \dots, 1000)$, $\Sigma = dI_d$. We also start the process on the equator, to emulate a situation where the prior and posterior modes are very far apart and the target is heavy tailed.

We present plots of the sample paths for the adaptive SRW, SSS, SBPS, and a plot of a HMC sample path struggling to find the modes for comparison. These are Figures 7, 8, 9 and 10 respectively. For our adaptation scheme, we use the latest half of the adaptive epochs to obtain an estimator for the target mean and covariance matrix via the standard empirical estimators. We also scale the covariance matrix to center the latest adaptive epoch's sample path around the equator. This scaling is included to control our estimators in the case where the target covariance may be infinite.

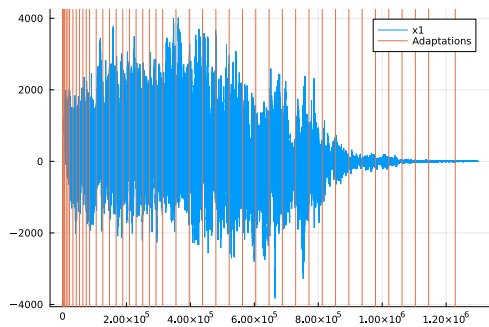


(a) Plot of the first coordinate X_1

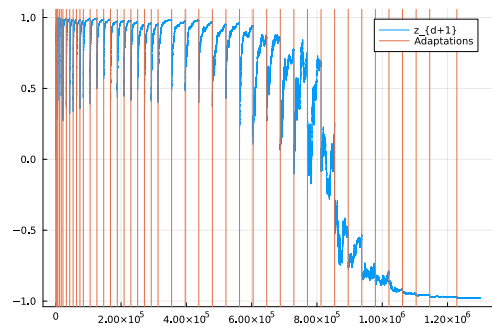


(b) Plot of the latitude Z_{d+1}

Figure 7: Adaptive SRW sample paths targeting a multivariate t -distribution with $\nu = 2$, $d = 200$, and initial parameters $\mu = (1000, \dots, 1000)$, $\Sigma = dI_d$. We set $h = 0.1d^{-1}$ throughout. This run took approximately 8 hours.

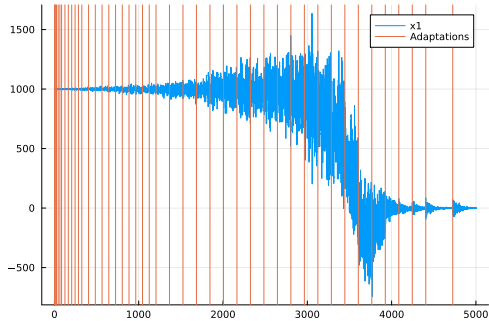


(a) Plot of the first coordinate X_1

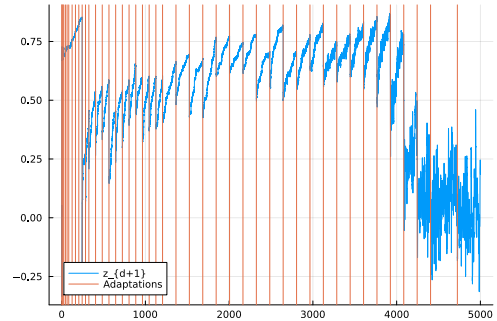


(b) Plot of the latitude Z_{d+1}

Figure 8: Adaptive SSS sample paths targeting a multivariate t -distribution with $\nu = 2$, $d = 200$, and initial parameters $\mu = (1000, \dots, 1000)$, $\Sigma = dI_d$. This run took approximately 10 minutes.

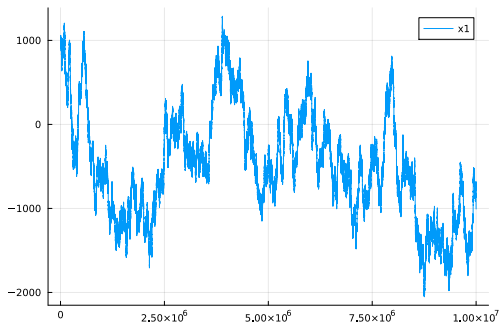


(a) Plot of the first coordinate X_1

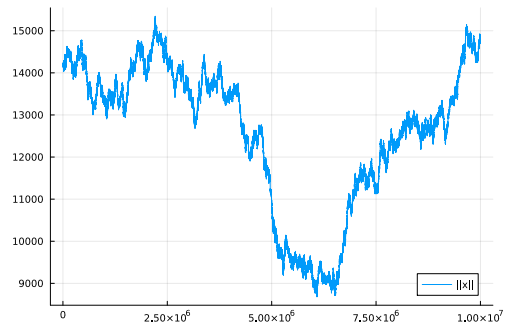


(b) Plot of the latitude Z_{d+1}

Figure 9: Adaptive SBPS sample paths targeting a multivariate t -distribution with $\nu = 2$, $d = 200$, and initial parameters $\mu = (1000, \dots, 1000)$, $\Sigma = dI_d$. We set $\lambda_{\text{ref}} = 1$ throughout. This run took approximately 60 minutes, but the last two adaptive epochs (15% of the run) took 75% of the time.



(a) Plot of the first coordinate X_1



(b) Plot of the norm $\|X\|$

Figure 10: HMC sample paths targeting a multivariate t -distribution with $\nu = 2$, $d = 200$, started at $x_0 = (1000, \dots, 1000)$. This run took approximately 3.5 hours.

The HMC sample path in Figure 10 was essentially unable to make any progress in finding the mode of the target distribution. This is to be expected when the tails of the distribution are so heavy and the dimension is relatively large.

In all cases the first thing the stereographic algorithms do is to gradually make their way towards N , then expand the radius of the sphere through the adaptation scheme, then continue going towards N (this can be seen by the plots of the trajectories of Z_{d+1}). However, in the x_1 path, this exploration leads to oscillations more or less symmetrically around the initial parameter μ .

The algorithms then take varying lengths of time to find the true mean of the target distribution (the SBPS takes a long time to expand the radius, but then finds the mean very quickly, as seen in Figure 9a, whereas the SRW or SSS expands the radius very quickly, then requires a long time to find the mean, as in Figure 7a or 8a). Once the mean is found, they are able to stay there and adapt the μ parameter to recenter the sphere around the true mean. The process then drops down from the North pole, but may now need a long time to shrink the Σ parameter back down to match the target. This behaviour is clearly seen in the SRW or SSS, where the z_{d+1} path suddenly drops from 1 to -1 in Figure 7b or 8b.

When comparing the SRW and SSS, we found that the SSS has two key benefits. First of all, it is significantly faster both in computational terms and algorithmic terms. It took the SRW about 8 hours to run this toy example, whereas it only took the SSS 10 minutes. Furthermore, we can see that the number of steps in each phase of the SSS is much lower than for the SRW. Secondly, the SSS is only parametrised by μ and Σ , for which we have very explicit guidance. The SRW also includes the step size parameter h , which has implicit guidance for tuning when μ and Σ are optimally chosen, but no advice as to how to tune it while we are still adapting those parameters. For these two reasons, we recommend using the adaptive SSS over the adaptive SRW. However, we must note that a single step of SSS will take much more computational effort in the shrinkage step than a single step of SRW in cases where the particle is in a very small spike of probability density.

When comparing the SSS to the SBPS, it is noteworthy that PDMPs in general are more complicated to simulate. The Poisson thinning step (see Corbella, Spencer, and Roberts 2022 for details) is quite sensitive to certain parameters, and could probably be significantly accelerated. In particular, when the target π_γ is focused around a small region, or becomes highly heterogeneous, the bounce rate explodes and requires many bounce events in order to keep the particle near the mode. Our current conjecture for the slowdown seen in Figure 9 is that, whilst moving the μ parameter, the process enters some heterogeneous scale regions and requires many bounce events to stay near the mode. We also must note our choice of refreshment rate $\lambda_{\text{ref}} = 1$ is completely arbitrary, and it is ongoing research to

see how SBPS's behaviour could improve as one varies the λ_{ref} .

Thus, although we found that the SBPS was computationally slower than the SSS, we feel that a more in depth discussion of the implementation of the SBPS is required to come to a verdict on relative computational efficiency. However, in the simpler cases such as targeting Gaussian or lighter tailed t -distributions with the correct choices of γ where uninformed proposals are often accepted, or scenarios where gradients are very expensive to evaluate, we expect the simpler SSS to always outperform the complicated SBPS.

By contrast, it is clear that the uninformed proposals in the SSS cause it to struggle to find the mode, whereas the SBPS is able to do so very quickly once it reaches the appropriate latitude. This then leads to a secondary advantage of the adaptive SBPS, since the shorter sample paths allow the adaptive parameters to more easily forget the initial search window and immediately place the probability mass on the equator. Furthermore, in scenarios where the target is not spherically symmetrical and gradient information becomes more relevant to the sampling problem, we expect the SBPS to outperform the SSS.

Thus, when choosing between using the SSS or SBPS, a user should consider:

- the computational efficiency of the user's implementation of the SBPS,
- the correctness of the initial parameters of the stereographic projection,
- the relative cost/benefit of using gradient information if the target is either expensive to evaluate, or essentially uniform around the equator.

As a closing remark on the simulations, we must point out that the parameters in each of our figures have definitely not converged. This can be seen since the SRW and SSS paths end near the South pole $-N$, and the SBPS path has to focus in on the mode after each of the last few adaptation steps. However, once the processes have reached the mode of the distribution, the empirical estimators for the sample mean and covariance will converge to the optimal values. It simply takes a long time for the history of the chain to be forgotten. Thus, for the sake of brevity, we only include the sample paths until the mode is reached.

3.4 Asymptotic Results

We now present our main results for the convergence of estimators using the adaptive stereographic algorithms. Given any bounded function $f : \mathbb{R}^d \rightarrow \mathbb{R}$, we want to estimate $\pi(f) = \mathbb{E}_\pi(f(X))$. We are interested in the behaviour of the estimators:

$$\widehat{f}_t^{\text{disc}} = \frac{1}{t} \sum_{s=0}^{t-1} f(X_s), \quad \widehat{f}_t^{\text{cont}} = \frac{1}{t} \int_{s=0}^t f(X_s) ds \quad (3.4)$$

depending on whether we are considering a continuous or discrete time algorithm. Note also that, for the sake of computation, we will generally evaluate estimators from SBPS sample paths by taking a discrete skeleton with small mesh size.

With this definition, it is clear why we need to move the path off of \mathbb{S}^d : since f is fixed on \mathbb{R}^d , we have to move our theory onto the projections of the sample paths in Euclidean space. Otherwise, the target function would be:

$$f_\gamma(z) = f(\text{SP}_\gamma^{-1}(x)), \quad (3.5)$$

which changes as we update γ .

To get LLNs and a CLT for the AIR stereographic algorithms, we make several assumptions.

Assumption 3.1. *The adaptation scheme for the parameter updates keeps $\gamma_i = (\mu_i, \Sigma_i)$ in the compact set $\Gamma_{r,R}$ for all i , where:*

$$\Gamma_{r,R} = \{\gamma \in \Gamma : \|\mu\| \leq R, r^2 \leq \rho_i \leq R^2, \forall i\},$$

for $0 < r < R$, and ρ_i are the eigenvalues of Σ .

For the AIR SRW, also assume $r \leq h_i \leq R$ for each h_i . For the AIR SBPS, also assume $r \leq \lambda_i \leq R$ for each λ_i .

This assumption restricts the parameters to a compact set, so that even if the adaptation scheme goes “wrong”, we can control how poorly the estimators behave. In particular, we can use any estimator for our parameters which respect Assumption 3.1, and we will not require trickier conditions such as diminishing adaptations for our WLLN or SLLN.

Assumption 3.2. *The adaptation lags $t_k = \Theta(k^\beta)$ are chosen under mild conditions.*

This assumption allows the AIR setup to be used. The mild additional conditions arise through our method of proving the results and are simply a condition on the expression for the times t_k . These are of very little practical relevance, and we conjecture that simply assuming $t_k = \Theta(k^\beta)$ is sufficient. See Appendix A.2 for more details.

For our necessary assumptions on the target distribution, we will need a slightly different assumption for the SRW and SSS to the assumption for the SBPS. For the SRW and SSS, we need:

Assumption 3.3. *The target density π is positive, continuous and satisfies:*

$$\limsup_{\|x\| \rightarrow \infty} \left(\pi(x) (\|x\|^2 + 1)^d \right) < \infty.$$

This assumption ensures that π_γ is bounded over \mathbb{S}^d . Our Markov chains are then targeting a distribution with a bounded density and a compact support, leading to naturally strong convergence properties. If this condition fails, the chains could get stuck in the vicinity of the North pole for arbitrarily long times.

Note that this condition is satisfied for distributions with relatively heavy tails, such as multivariate t -distributions with at least d degrees of freedom.

Since the SBPS works off of $\nabla_z \log \pi_\gamma$, we need a different condition:

Assumption 3.4. *The target density π is positive, continuously differentiable and satisfies:*

$$\limsup_{\|x\| \rightarrow \infty} \left(x \cdot \nabla_x \log \pi(x) + R \|\nabla_x \log \pi(x)\| \right) + 2d < \frac{1}{2},$$

for some $R > 0$.

This assumption also ensures that the North pole does not become an inescapable singularity. It is also satisfied for distributions with relatively heavy tails, such as multivariate t -distributions with more than $d - \frac{1}{2}$ degrees of freedom.

Note that both Assumption 3.3 and Assumption 3.4 fail in the example discussed in Section 3.3 (a multivariate t -distribution with $d = 200$, $\nu = 2$). Thus, although these are sufficient conditions to expect good convergence results, we do not require them for the algorithms to still perform well, and significantly outperform non-stereographic counterparts.

With these assumptions, we can then obtain the following result on the behaviour of \widehat{f}_t :

Theorem 3.5 (Asymptotics of \widehat{f}_t). *Consider either of the estimators \widehat{f}_t as given in Equation (3.4) for a bounded function $f : \mathbb{R}^d \rightarrow \mathbb{R}$, applied to the AIR SRW, SSS, SBPS, or a discrete skeleton of the SBPS, targeting the distribution π on \mathbb{R}^d .*

Under assumption 3.1 for any $r < R \in (0, \infty)$, assumption 3.2 for $\beta > 0$, and either assumption 3.3 if we are working with the SRW or SSS, or assumption 3.4 for the SBPS, then for any initial position or parameters:

- For any $\beta > 0$,

$$\mathbb{E}_{(x,w)}^{\gamma_0} \left([\widehat{f}_t - \pi(f)]^2 \right) \xrightarrow{\mathcal{L}^2} 0, \quad \text{as } t \rightarrow \infty$$

so that a WLLN holds.

- For $\beta > \frac{1}{2}$, a SLLN holds: $\widehat{f}_t \xrightarrow{a.s.} \pi(f)$ as $t \rightarrow \infty$.
- For $\beta > 1$, if $\gamma_i \xrightarrow{P} \gamma_\infty$, for some constant γ_∞ , such that the asymptotic variance $\sigma^2(\gamma_\infty) > 0$, and that $\sigma^2(\gamma)$ is a continuous function of γ , a CLT holds:

$$\sqrt{t}(\widehat{f}_t - \pi(f)) \xrightarrow{D} \mathcal{N}\left(0, \sigma^2(\gamma_\infty)\right), \quad \text{as } t \rightarrow \infty.$$

Note that, although we express this in a unified way, the asymptotic variance $\sigma^2(\gamma)$ will depend on the choice of algorithm. Additionally, convergence of γ_i to some constant γ_∞ is given by part (a) of the theorem if we are using bounded empirical estimates for the optimal values of μ and Σ , as guided by Equation (3.2).

Comparing this result to other similar results, such as those discussed in Roberts and Rosenthal 2007, we see that under significantly weaker assumptions on the adaptation scheme, we obtain a WLLN and SLLN. The additional requirement on the convergence of the parameter and continuity of the asymptotic variance in the CLT result are indeed stronger, but they are comparable to those found in any similar result. We do not present a result on the ergodicity of the algorithm, i.e. whether $X_t \xrightarrow{D} \pi$ as $t \rightarrow \infty$, as these would bring identical conditions to more general results already found in the literature (Roberts and Rosenthal 2007).

Although the sampling mechanisms for our three algorithms are very different, we obtain essentially identical convergence results. This is an artifact of our proof, in which we use the simultaneous uniform ergodicity of the processes to create a unifying auxiliary Markov chain which is much easier to work with than any of our original processes.

4 The Segment Chain for Uniformly Ergodic Markov Processes

We have already discussed the AIR framework and its intuitive appeal. However, the theory presented assumes a discrete time chain, with a 1-step small set condition and simultaneous geometric ergodicity, which we do not explicitly have in our cases. Instead, the stereographic algorithms are all simultaneously uniformly ergodic, and the SBPS lives in continuous time.

In this section, we present a novel auxiliary process, the segment chain, which gives a unified framework for analysing any uniformly ergodic Markov process. This framework is particularly useful for the study of continuous time chains where notions of splitting, excursions and regenerations are not as well studied.

4.1 A Markov chain in the space of paths

Consider a continuous time Markov process $\{X_t\}_{t \geq 0}$ on a sample space χ and its parametrised associated transition semigroup $\{P_\gamma^t\}_{t \geq 0}$, where $\gamma \in \Gamma$ is a parameter. Let π_γ be the stationary measure of P_γ (these need not be equal). Unfortunately, this notation clashes with the π_γ from the stereographic projection, and these two do not necessarily equate in our setting. For example, for the SBPS, this stationary

distribution would be the joint distribution of X in \mathbb{R}^d and some latent velocity component whose distribution depends on γ . More on this later.

Suppose the process satisfies a minorisation condition of the form:

$$P_\gamma^T(x, \cdot) \geq \epsilon \nu(\cdot), \quad \forall x \in \chi, \quad (4.1)$$

with $T > 0$, $\epsilon > 0$, and ν a probability measure ν on χ all independent of γ . The existence of such a condition is equivalent to uniform ergodicity of the process, and suggests that regardless of the values of X_t or γ , we have probability ϵ to get $X_{t+T} \sim \nu$ independently of $\{X_s\}_{0 \leq s \leq t}$.

We then define the segment chain $\{\Phi_n\}_{n \in \mathbb{N}}$ to be a discrete time Markov chain with $\Phi_n : [0, T] \rightarrow \chi$ such that:

$$\Phi_n(t) = X_{nT+t}. \quad (4.2)$$

The segment chain $\{\Phi_n\}_{n \in \mathbb{N}}$ is then a Markov chain in the space of functions from $[0, T]$ to χ , which we shall simply call Ω .

If we have a discrete time Markov chain satisfying the minorisation condition (4.1), we can instead take:

$$\Phi_n(t) = X_{nT+\lfloor t \rfloor}, \quad (4.3)$$

to obtain the segment chain.

The crucial observation is that, using the minorisation condition (4.1), we can “split” the chain $\{\Phi_n\}_{n \in \mathbb{N}}$ such that, in a way we shall make rigorous later, for each n , with probability ϵ we have $\Phi_{n+1}(0) \sim \nu$ independently of $\Phi_0, \dots, \Phi_{n-1}$. This will allow us to divide sample paths into weakly dependent, identically distributed blocks, to which we can then apply standard techniques to get our LLNs and CLT results.

For further details on splitting techniques for discrete time Markov chains, see Meyn and Tweedie 2012, Sections 5 and 17.

4.2 Simultaneous Uniform Ergodicity

Before going any further, we must ensure that our algorithms satisfy a minorisation condition as described in Equation (4.1).

Since the stereographic Markov processes live in \mathbb{S}^d , which is compact, it is natural for them to exhibit uniform ergodicity properties similar to those of other algorithms targeting bounded densities with compact supports. As discussed alongside assumptions 3.3 and 3.4, the situation becomes slightly more complicated at the North pole N , since $\pi_\gamma(z)$ or $v \cdot \nabla_z \log \pi_\gamma(z)$ may not remain bounded as $z_{d+1} \rightarrow 1$.

Indeed, we have the following results for the SRW and SSS:

Lemma 4.1 (SRW Minorisation Condition). *Suppose that $\gamma \in \Gamma_{r,R}$ for $0 < r < R < +\infty$. For P the Markov transition kernel for the SRW targeting π , and assuming π satisfies assumption 3.3, then $\exists \epsilon > 0$ and a probability measure ν on \mathbb{R}^d such that $\forall x \in \mathbb{R}^d$:*

$$P^3(x, \cdot) \geq \epsilon \nu(\cdot).$$

Furthermore, ϵ and ν can be chosen to be independent of γ .

Lemma 4.2 (SSS Minorisation Condition). *Suppose that $\gamma \in \Gamma_{r,R}$ for $0 < r < R < +\infty$. For P the Markov transition kernel for the SSS targeting π , and assuming π satisfies assumption 3.3, then $\exists \epsilon > 0$ and a probability measure ν on \mathbb{R}^d such that $\forall x \in \mathbb{R}^d$:*

$$P(x, \cdot) \geq \epsilon \nu(\cdot).$$

Furthermore, ϵ and ν can be chosen to be independent of γ .

Note that ϵ and ν are implicitly different for the SRW and SSS. The proofs of these results involve constructing suitable sequences of events which allow the process to hit a given open ball of arbitrarily small radius, then bounding the probability of this sequence of events. We can then extend this lower bound to a measure on $(\mathbb{R}^d, \mathcal{B}(\mathbb{R}^d))$ by writing any set $A \in \mathcal{B}(\mathbb{R}^d)$ as a union of open balls. Most of the details can be found in Yang, Łatuszyński, and Roberts 2022 for the SRW or Habeck et al. 2023 for the SSS.

For the equivalent result in the case of the SBPS, we project the sample path $\{Z_t, V_t\}_{t \geq 0}$ onto Euclidean space, we obtain a Markov process $\{X_t, W_t\}_{t \geq 0}$ with invariant distribution $\pi(x) \times p_\gamma(w|x)$ over $\mathbb{R}^d \times \mathbb{S}^{d-1}$. W_t is a unit vector related to the direction of the particle in \mathbb{R}^d , and is only necessary because $\{X_t\}_{t \geq 0}$ is not a Markov process.

Note importantly that in this setting, we are indeed considering a stationary distribution which changes with the parameter.

Lemma 4.3 (SBPS Minorisation Condition). *Suppose that $\gamma \in \Gamma_{r,R}$ for $0 < r < R < +\infty$. For P the Markov transition kernel for the projected SBPS process $\{(X_t, W_t)\}_{t \geq 0}$ targeting π , and assuming π satisfies assumption 3.4, then $\exists T^* > 0$, $\epsilon > 0$ and a probability measure ν on $\mathbb{R}^d \times \mathbb{S}^{d-1}$ such that, $\forall T \geq T^*$, $\forall (x, w) \in \mathbb{R}^d \times \mathbb{S}^{d-1}$:*

$$P^T((x, w), \cdot) \geq \epsilon \nu(\cdot).$$

Furthermore, T^ , ϵ and ν can be chosen to be independent of γ .*

The proof of Lemma 4.3 follows a Lyapunov function and small set proof. Most of the details can be found in Yang, Łatuszyński, and Roberts 2022. Note that Lemma 4.3 gives a minorisation condition for the continuous time SBPS, as well as any discrete time skeleton of the SBPS.

With these minorisation conditions, we can map any of our algorithms' sample paths onto a segment chain with identical properties. We therefore only need to prove results in the general setting to obtain results for each of our algorithms, under appropriate conditions on π .

Additionally, since our Lemmas hold simultaneously over all $\gamma \in \Gamma_{r,R}$, we can use them to control the behaviour of an adaptive algorithm in which we vary the parameters as we run the process.

4.3 Splitting and Regenerations for the segment chain

We now return to our segment chain $\{\Phi_n\}_{n \in \mathbb{N}}$, as described in either Equation (4.2) or (4.3) for a general (continuous or discrete time) Markov process X on a state space χ .

We let $\mathbb{Q}_\mu(\cdot; \gamma)$ be the probability measure on $(\Omega, \mathcal{B}(\Omega))$, the space of paths of length T , induced by the dynamics of X under parameter γ , subject to $X_0 \sim \mu$ for some probability measure μ on χ . If $X_0 = x$ a.s., we write this measure as $\mathbb{Q}_x(\cdot; \gamma)$. With this setup, we have that $\forall A \in \mathcal{B}(\Omega), n \in \mathbb{N}$:

$$\mathbb{P}(\Phi_n \in A | \Phi_{0:(n-1)}) = \mathbb{Q}_{\Phi_{n-1}(T)}(A; \gamma). \quad (4.4)$$

We write:

$$P_{\Phi; \gamma}(\phi, \cdot) = \mathbb{Q}_{\phi(T)}(\cdot; \gamma), \quad (4.5)$$

for its transition kernel. If π_γ is the unique stationary distribution of X , this kernel admits $\mathbb{Q}_{\pi_\gamma}(\cdot; \gamma)$ as its stationary distribution.

We hope to use minorisation condition (4.1) to extend the state space Ω to a new space $\check{\Omega} = \Omega \times \{0, 1\}$. We construct a Markov chain $(\Phi_n, Y_n)_{n \in \mathbb{N}}$ on $\check{\Omega}$ which possesses an ergodic atom, such that the marginal transition probabilities of the Φ component have a transition kernel satisfying Equation (4.4).

Mimicking the split chain constructions from Bednorz, Łatuszyński, and Latala 2008 or Meyn and Tweedie 2012, Section 17.3, we start by considering the T -skeleton chain for the original process $\{X_{nT}\}_{n \in \mathbb{N}}$. Given the minorisation (4.1), we can define $Y_n \in \{0, 1\}$, and obtain a Markov chain $\{(X_{nT}, Y_n)\}_{n \in \mathbb{N}}$ with associated probability measure $\check{\mathbb{P}}_\gamma$ by setting:

$$\begin{aligned} \check{\mathbb{P}}_\gamma(X_{(n+1)T} \in A | Y_n = 1, X_{nT}) &= \nu(A), \\ \check{\mathbb{P}}_\gamma(X_{(n+1)T} \in A | Y_n = 0, X_{nT}) &= \eta_\gamma(X_{nT}, A), \end{aligned} \quad (4.6)$$

where

$$\eta_\gamma(x, A) = \frac{P_\gamma^T(x, A) - \epsilon \nu(A)}{1 - \epsilon}, \quad (4.7)$$

as well as:

$$\check{\mathbb{P}}_\gamma(Y_n = 1 | X_{nT}) = \epsilon. \quad (4.8)$$

It is a standard result that this chain has the correct marginal distributions for $\{X_{nT}\}_{n \in \mathbb{N}}$, and that the set $\chi \times \{1\}$ is a regenerative atom for the chain, i.e. $A \subset \chi, i \in \{0, 1\}$:

$$\check{\mathbb{P}}_\gamma(X_{(n+1)T} \in A, Y_{n+1} = i | X_{nT}, Y_n = 1) = \nu(A)\epsilon^i(1 - \epsilon)^{1-i}. \quad (4.9)$$

In other words, conditionally on $\{Y_n = 1\}$, the processes $\{X_{kT}, Y_k\}_{k \geq n+1}$ and $\{X_{kT}, Y_k\}_{k \leq n}$ are independent.

To transfer these properties over to the segment chain Φ , we bridge the paths from X_{nT} to $X_{(n+1)T}$ conditionally on the endpoints. We define the Radon-Nykodym derivatives $\frac{d\nu}{dP_\gamma^T}$ and $\frac{d\eta_\gamma}{dP_\gamma^T}$, which are functions of x and x' , and extend the measure $\check{\mathbb{P}}_\gamma$ to be a transition kernel from Φ_n to Φ_{n+1} . For the Y_n updates, we get:

$$\check{\mathbb{P}}_\gamma(Y_n = 1 | \{\Phi_k\}_{k=0}^n, \{Y_k\}_{k=0}^{n-1}) = \epsilon, \quad (4.10)$$

and for the Φ_{n+1} updates, we get:

$$\begin{aligned} \check{\mathbb{P}}_\gamma(\Phi_{n+1} \in A | Y_n = 1, \Phi_n) &= \int_A \frac{d\nu}{dP_\gamma^T}(\Phi_n(T), \phi(T)) d\mathbb{Q}_{\Phi_n(T)}(\phi; \gamma), \\ \check{\mathbb{P}}_\gamma(\Phi_{n+1} \in A | Y_n = 0, \Phi_n) &= \int_A \frac{d\eta_\gamma}{dP_\gamma^T}(\Phi_n(T), \phi(T)) d\mathbb{Q}_{\Phi_n(T)}(\phi; \gamma). \end{aligned} \quad (4.11)$$

One can check that these give the appropriate marginal transition kernels to recover $\Phi_{n+1} \sim \mathbb{Q}_{\Phi_n(T)}(\cdot; \gamma)$. It is easy to check that the invariant distribution for the split segment chain is:

$$\check{\pi}_\gamma(A \times \{i\}) = \epsilon^i(1 - \epsilon)^{1-i} \mathbb{Q}_{\pi_\gamma}(A; \gamma), \quad (4.12)$$

for $A \in \mathcal{B}(\Omega)$.

Let $\check{P}_\gamma((\phi, y), \cdot)$ be the transition kernel of the split segment chain $\{\Phi_n, Y_n\}_{n \in \mathbb{N}}$, as given by Equations (4.11) and (4.10). Since, $Y_n = 1$ implies that $X_{(n+1)T} \sim \nu$ independently of the history of the process up to time Tn , we can show that the split segment chain admits $\check{\alpha} = \Omega \times \{1\}$ as an atom:

Lemma 4.4 (Atom for the Split Segment Chain). *For $\{\Phi_n, Y_n\}_{n \in \mathbb{N}}$ the split segment chain with transition law \check{P}_γ , we have that $\forall \phi \in \Omega$, and $\forall A \in \mathcal{B}(\Omega)$, $i \in \{0, 1\}$:*

$$\check{P}_\gamma^2((\phi, 1), A \times \{i\}) = C^i(1 - C)^{1-i} \mathbb{Q}_\nu(A; \gamma).$$

In particular, conditionally on the event $\{Y_n = 1\}$, the pre- n process $\{\Phi_k, Y_k\}_{k \leq n}$ and the post- $(n+2)$ process $\{\Phi_k, Y_k\}_{k \geq n+2}$ are independent. Given $\{Y_n = 1\}$, $\{\Phi_k, Y_k\}_{k \geq n+2}$ has the same law as $\{\Phi_k, Y_k\}_{k \geq 1}$ with initial distributions $\Phi_0(T) \sim \nu$ and $Y_0 \sim \text{Bern}(C)$.

With Lemma 4.4, we can consider an excursion process between hitting times of the atom $\check{\alpha}$, the details of which can be found in Appendix A.1. These are identically distributed, 1-dependent sequences of random (Geom(ϵ) distributed) length. This structure can be visualised in Figure 11.

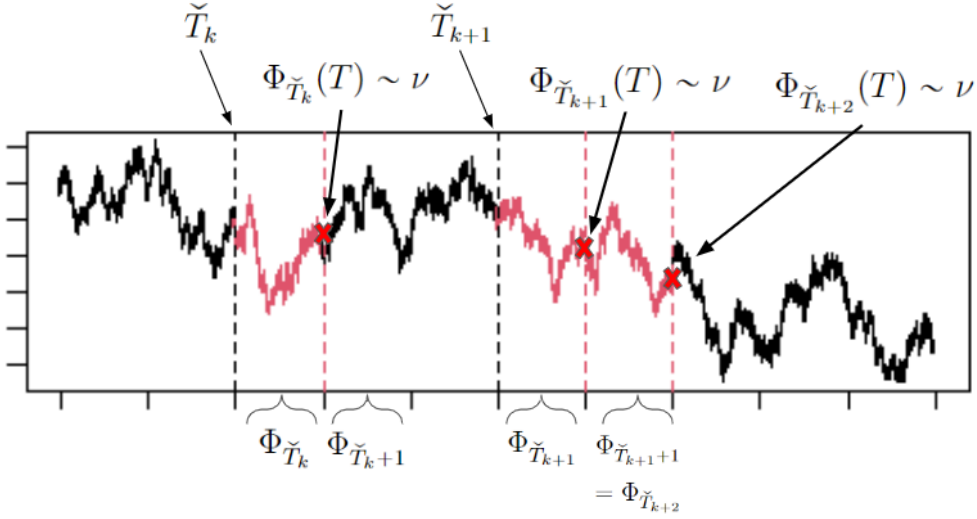


Figure 11: Example path including excursions (path is for illustration purposes and does not reflect a real sampling scheme). The regeneration times \check{T}_k (defined in appendix A.1) are shown, along with associated random variables: the regeneration segments $\Phi_{\check{T}_k}$ are shown in red. These segments are independent of neither the immediate past, nor the immediate future. The random length excursions Ψ_k go between red crosses and are identically distributed and 1-dependent.

With this framework, any uniformly ergodic Markov process can be transformed into a discrete time chain with an ergodic atom.

4.4 Proving the Asymptotic Results

We have now got enough setup to prove the results in Theorem 3.5. Consider a bounded function $f : \mathbb{R}^d \rightarrow \mathbb{R}$, with $|f| \leq M$, and assume that $\pi_\gamma f = 0$ for all $\gamma \in \Gamma$. We are interested in the behaviour of the estimator \hat{f}_t as given in Equation

(3.4). If the original process X is a continuous time process, we write:

$$F(\phi) = \frac{1}{T} \int_{s=0}^T f(x_s) ds, \quad (4.13)$$

for $\phi = \{x_s\}_{s=0}^T \in \Omega$, to get that:

$$\widehat{f}_t = \frac{1}{n} \sum_{i=0}^{n-1} F(\Phi_i) + \mathcal{O}(t^{-1}), \quad (4.14)$$

where $n = \lfloor \frac{t}{T} \rfloor$. An analogous statement can be made for discrete time processes. The asymptotic properties of \widehat{f}_t will be the same as those of:

$$\widehat{f}_n^\Phi = \frac{1}{n} \sum_{i=0}^{n-1} F(\Phi_i), \quad (4.15)$$

as $n \rightarrow +\infty$.

Recall that we will be working with an adaptive MCMC scheme where the lags between adaptation times are polynomially increasing. Let $\beta > 0, c \geq 1$ such that $\forall k \in \mathbb{N}$:

$$\frac{1}{c} k^\beta \leq n_k \leq c k^\beta, \quad (4.16)$$

for $n_k \in \mathbb{N}$. The adaptation times are then given by $N_k = \sum_{i=1}^k n_k$, with $N_0 = n_0 = 0$ for consistency of notation.

We consider the AIR segment chain process as follows: let $\{(\Phi_n, Y_n)\}_{n \in \mathbb{N}}$ evolve according to \check{P}_{γ_k} for $N_k \leq n < N_{k+1}$, then update the parameter to γ_{k+1} at N_{k+1} . Then we obtain the following results:

Theorem 4.5 (AIR Segment Chain Asymptotic Results). *Consider $(\Phi_n, Y_n)_{n \geq 0}$ the AIR segment chain process, where the original family of transition kernels $\{P_\gamma\}_{\gamma \in \Gamma}$ have invariant distributions π_γ and satisfy the minorisation condition (4.1). Assume that f is bounded and $\mathbb{E}_{\pi_\gamma}(f(X)) = 0$ for all $\gamma \in \Gamma$. Then $\forall (\Phi_0, Y_0) \in \check{\Omega}, \gamma_0 \in \Gamma$, and any adaptation scheme:*

- For any $\beta > 0$,

$$\mathbb{E}_{(\Phi_0, Y_0)}^{\gamma_0} \left((\widehat{f}_n^\Phi)^2 \right) \xrightarrow{\mathcal{L}^2} 0, \quad \text{as } n \rightarrow \infty$$

so that a WLLN holds.

- For $\beta > \frac{1}{2}$, a SLLN holds: $\widehat{f}_n^\Phi \xrightarrow{a.s.} 0$ as $n \rightarrow \infty$.

- For $\beta > 1$, if $\gamma_i \xrightarrow{P} \gamma_\infty$ such that $\sigma^2(\gamma_\infty) > 0$, and that $\sigma^2(\gamma)$ is a continuous function of γ , then a CLT holds:

$$\sqrt{n}\widehat{f}_n^\Phi \xrightarrow{D} \mathcal{N}(0, \sigma^2(\gamma_\infty)).$$

The proof of Theorem 4.5 is in appendix B.

Since $\widehat{f}_t = \widehat{f}_n^\Phi + \mathcal{O}(t^{-1})$, we can use Theorem 4.5 to immediately obtain the results on \widehat{f}_t in Theorem 3.5, which concludes our discussion of the asymptotic results for the adaptive stereographic MCMC algorithms.

5 Discussion

We have discussed the use of adaptive MCMC methods to automatically tune the parameters of stereographic MCMC algorithms. Alongside theoretical convergence results, we have demonstrated our algorithms' ability to adapt to the target distribution and improve sampling efficiency in problems far more challenging than those covered by the theorems. These examples highlight the power of the stereographic projection as a way of helping sample from heavy tailed distributions, since standard off-the-shelf methods (namely HMC) have great difficulty tackling these problems when they find themselves in the tails.

The theoretical results also provide insight into other potential uniformly ergodic algorithms: the segment chain framework can be used going forward to prove convergence results for any adaptive MCMC algorithm based on a simultaneously uniformly ergodic collection of Markov kernels.

All three stereographic algorithms are able to target high dimensional, heavy tailed target distributions, and we demonstrated their ability to tune parameters when started in the tails. In terms of their relative mixing properties in the stationary regime, we expect the SSS to outperform the other algorithms in simple settings where the target is spherically symmetric and can be essentially thought of as uniform over the equator. If the target distribution is somewhat irregular, the gradient information provided by the SBPS should allow it to outperform the SSS. In cases where the gradient is expensive to compute, or the target is highly irregular, we expect the SRW to inherit the robustness of the Euclidean RWM algorithm and potentially outperform the other algorithms if all the parameters are optimally chosen. However, in such cases one could also argue that the shrinkage proposal (Algorithm 2 or Figure 3) in the SSS becomes essentially equivalent to a RWM proposal once it rejects enough steps, so that the SSS can only perform so much worse to a suboptimally parametrised SRW.

We conclude this paper with several further avenues of research:

- *More Simulation Studies:* There is still much investigation required into the behaviour of the stereographic algorithms (adaptive or not) in cases where the target distributions are irregular. It would be of interest to do a more thorough overview of how the stereographic projection improves MCMC related analysis in real world applications where heavy tailed distributions arise.
- *SBPS Refreshment Rate:* Several results exist discussing the behaviour of the Euclidean BPS algorithm as one varies the refreshment rate λ_{ref} (Bierkens and Duncan 2017; Bierkens, Kamatani, and Roberts 2022). It would be of interest to analyse the SBPS using similar methods to better understand the implications of choices of λ_{ref} on the mixing properties of the algorithm.
- *Other Stereographic Algorithms:* We have seen that the stereographic projection naturally leads to uniformly ergodic algorithms, even when the target distribution is heavy tailed. It is therefore natural to consider stereographic versions of other commonly used algorithms, namely MALA or HMC, potentially following the works of Girolami and Calderhead 2011 on targeting distributions defined on Riemannian manifolds.
- *Generalising the Segment Chain:* Finally, though the segment chain is an elegant way of proving results when the underlying Markov kernels are uniformly ergodic, this is generally too strong an assumption. It is therefore of interest to see whether a segment chain framework could be used under weaker assumptions of geometric or polynomial ergodicity.

Acknowledgement: We would like to acknowledge the Engineering & Physical Sciences Research Council for their funding.

A Further details

A.1 Excursions of the segment chain

We discuss the regenerations and excursions of the split segment chain $\{(\Phi_n, Y_n)\}_{n \in \mathbb{N}}$.

As a follow-up remark, since $Y_n = 1$ implies that Φ_n and Φ_{n+2} are independent, we note that the “bridge” path Φ_{n+1} has the property that $\Phi_{n+1}(0) = \Phi_n(T)$ and $\Phi_{n+1}(T) = \Phi_{n+2}(0)$ are independent.

We will write ν^* for an arbitrary measure on $\check{\Omega}$ such that, for $A \in \mathcal{B}(\mathbb{R}^d \times \mathbb{S}^{d-1})$ and $i = 0, 1$:

$$\nu^*(\phi(T) \in A, Y = i) = \epsilon^i (1 - \epsilon)^{1-i} \nu(A), \quad (\text{A.1})$$

i.e., such that $\Phi \sim \nu^* \implies \Phi(T) \sim \nu$ and $Y \sim \text{Bern}(\epsilon)$.

Since the Y_n updates are not affected by the current position Φ_n , we can very easily identify the behaviour of our regeneration times. For $k \geq 1$, the hitting and return times of the atom are:

$$\begin{aligned} \check{\sigma}_1 &= \inf(n \geq 0 : Y_n = 1), & \check{\sigma}_k &= \inf(n > \check{\sigma}_{k-1} : Y_n = 1), \\ \check{\tau}_1 &= \inf(n \geq 1 : Y_n = 1), & \check{\tau}_k &= \inf(n > \check{\tau}_{k-1} : Y_n = 1). \end{aligned} \quad (\text{A.2})$$

Alongside Lemma 4.4, we can concisely write that $\{\Phi_l, Y_l\}_{l \geq \check{\sigma}_{k+2}}$ has the same law as $\{\Phi_k, Y_k\}_{k \geq 1}$ started from $(\Phi_0, Y_0) \sim \nu^*$.

Thanks to uniform ergodicity, we can obtain the following explicit result on the distribution of the delayed renewal sequence $\{\check{\sigma}_k\}_{k \in \mathbb{N}}$.

Lemma A.1 (Return Times to the Atom). *For $\{\Phi_n, Y_n\}_{n \in \mathbb{N}}$ the split segment chain with transition law \check{P}_γ , let $\{\check{\sigma}_k\}_{k \in \mathbb{N}}$ be as given in Equation (A.2). Then the inter-arrival times $\check{\sigma}_{n+1} - \check{\sigma}_n$ for $n \geq 1$ are iid $\text{Geom}(\epsilon)$ random variables.*

Note in particular that since ϵ does not depend on γ , neither does the distribution of the inter-arrival times.

Finally, we can define the notion of excursions from the atom, allowing us to divide sample paths into 1-dependent, identically distributed blocks. It is convenient to define the regeneration times:

$$\check{T}_k = \check{\sigma}_k + 1, \quad (\text{A.3})$$

such that $\Phi_{\check{T}_k}(T) \sim \nu$ independently of $\{\Phi_n\}_{n \leq \check{\sigma}_k}$ (and also of $\Phi_{\check{T}_k}(0) = \Phi_{\check{\sigma}_k}(T)$), and so $\Phi_{\check{T}_k+1} \sim \mathbb{Q}_\nu(\cdot; \gamma)$ independently of the pre- $\check{\sigma}_k$ process, as in Lemma 4.4.

For $k \geq 0$, we define the excursion paths:

$$\Psi_k = \{\Phi_n, Y_n\}_{n=\check{T}_k+1}^{\check{T}_{k+1}}, \quad (\text{A.4})$$

These are random sequences in Ω of a.s. finite length, starting from $\Phi_{\check{T}_k+1}(0) = \Phi_{\check{T}_k}(T) \sim \nu$, and ending with $\Phi_{\check{T}_{k+1}}(T) \sim \nu$. By the above discussion, we can see that the variables $\{\Psi_k\}_{k \in \mathbb{N}}$ are identically distributed and 1-dependent. See Figure 11 for a visualisation of how \check{T}_k , Φ_n , ν , and Ψ_k all fit together.

We can use Bednorz, Łatuszyński, and Latala 2008, Lemma 5.2, alongside the minorisation condition (4.1), to find the distribution of $\Phi_{\check{\sigma}_k}(T)$.

Lemma A.2 (Stationarity at Renewal Times). *For ν and η_γ as defined in Equation (4.1) and Equation (4.7), we have that the unique stationary distribution π_γ of the original process X is given by:*

$$\pi_\gamma(\cdot) = \epsilon \sum_{n=1}^{\infty} (1 - \epsilon)^n \nu \eta_\gamma^{n-1}(\cdot).$$

As an immediate consequence, we get that $\Phi_{\check{\sigma}_k}(T) \sim \pi_\gamma$, for every $k \geq 2$.

The first statement is exactly Lemma 5.2 from Bednorz, Łatuszyński, and Latala 2008, but with our notation. The distribution of $\Phi_{\check{\sigma}_k}(T)$ then follows from the geometric distribution of $\check{\sigma}_k - \check{\sigma}_{k-1}$.

A.2 Assumptions on the Adaptation Times

Recall that in assumption 3.2, we included “mild conditions” on the adaptation lags t_k . These additional conditions arise via the construction of the segment chain $\{\Phi_n\}_{n \in \mathbb{N}}$ featuring in our proofs. Since we wish to run the AIR framework on the discrete time Markov process formed of segments of length T , it follows that we must adapt at integer multiples of T , so that $t_k = T \times n_k$.

Thus, we see that we will require the lags in Theorem 3.5 to have a common divisor, at least for large k . This condition can be difficult to satisfy if T is unknown, as is the case for the SBPS. Fortunately, since the minorisation condition (4.1) still holds if you increase T , we can consider a sequence of lags t_k such that $\lim_{k \rightarrow \infty} (\gcd(\{t_j : j \geq k\})) = \infty$, such as:

$$t_k = \inf(2^n : 2^n \geq k^\beta). \tag{A.5}$$

One can check that $t_k = \Theta(k^\beta)$, whilst having increasingly large common divisors. We can then apply the segment chain results once $t_k \geq T$, and consider the first part of the chain as asymptotically irrelevant.

B Proof of Theorem 4.5

In this section, we prove our main result, Theorem 4.5. We do this by bringing together the 1-dependent, identically distributed excursions Ψ_k discussed in Appendix A.1 and control the variance of our estimators.

For $i \in \mathbb{N}$, we define the Markov chain $\{H_j^{(i)}\}_{j \in \mathbb{N}}$ to have transition kernel \check{P}_{γ_i} , such that:

$$H_j^{(i)} = (\Phi_{N_i+j}, Y_{N_i+j}), \quad (\text{B.1})$$

for $j = 0, \dots, n_{i+1} - 1$, and $H_j^{(i)}$ evolves independently of $\{(\Phi_n, Y_n)\}_{n \geq N_{i+1}}$ for $j \geq n_{i+1}$.

As in Chimisov, Latuszyński, and Roberts 2018, Section 7, we let:

$$s_i = \sum_{j=N_i}^{N_{i+1}-1} F(\Phi_j) = \sum_{j=0}^{n_{i+1}-1} F(H_j^{(i)}), \quad (\text{B.2})$$

where we abuse notation slightly and set $F(\phi, y) = F(\phi)$. Next, we let:

$$\begin{aligned} \sigma_1^{(i)} &= \inf(j \geq 0 : H_j^{(i)} \in \check{\alpha}), & \sigma_{k+1}^{(i)} &= \inf(j > \sigma_k^{(i)} : H_j^{(i)} \in \check{\alpha}), \\ T_k^{(i)} &= \sigma_k^{(i)} + 1, \end{aligned} \quad (\text{B.3})$$

for $k \geq 1$ be the regeneration times for the $H^{(i)}$ process, defined analogously to \check{T}_k in (A.3). We can therefore write these excursions as:

$$\Psi_j^{(i)} = \{H_n^{(i)}\}_{n=T_j^{(i)}+1}^{T_{j+1}^{(i)}}. \quad (\text{B.4})$$

By Lemma 4.4, these excursions are identically distributed for i fixed and, conditionally on γ_i , they are 1-dependent.

We also define:

$$L_i = \inf(l \geq 1 : T_l^{(i)} \geq n_{i+1} - 1) = 1 + \sum_{j=0}^{n_{i+1}-2} \mathbb{1}(H_j^{(i)} \in \check{\alpha}), \quad (\text{B.5})$$

such that the last excursion of $H^{(i)}$ to start before we decouple from (Φ, Y) ends at step $T_{L_i}^{(i)}$.

Finally, we can define the sums over excursions which we will be analysing:

$$\begin{aligned} \eta_i &= \sum_{j=0}^{T_1^{(i)}} F(H_j^{(i)}), & \xi_i &= \sum_{j=T_1^{(i)}+1}^{T_{L_i}^{(i)}} F(H_j^{(i)}) \\ \zeta_i &= \sum_{j=n_{i+1}}^{T_{L_i}^{(i)}} F(H_j^{(i)}), & \xi_{i,j} &= \sum_{m=T_j^{(i)}+1}^{T_{j+1}^{(i)}} F(H_m^{(i)}). \end{aligned} \quad (\text{B.6})$$

For fixed i , since $\xi_{i,j}$ are functions of $\Psi_j^{(i)}$ only, these are identically distributed, 1-dependent (conditionally on γ_i) random variables.

With these, we get that:

$$s_i = \sum_{j=N_i}^{N_{i+1}-1} F(\Phi_j) = \eta_i + \xi_i - \zeta_i. \quad (\text{B.7})$$

η_i is a function of the $H^{(i)}$ path up until the first regeneration, and ζ_i is a function of the $H^{(i)}$ path from the point where we decouple from (Φ, Y) to the next regeneration. For large i , the vast majority of the sample path will be within the ξ_i term. The majority of the asymptotic results will then follow by studying $\xi_i = \sum_{j=1}^{L_i-1} \xi_{i,j}$, with $\xi_{i,j}$ identically distributed, conditionally 1-dependent random variables.

For the empirical sums $S_N = \sum_{j=0}^{N-1} F(\Phi_j)$, we can find $k = k(N)$ such that $N_k \leq N < N_{k+1}$ and write:

$$\begin{aligned} S_N &= \sum_{i=0}^k s_i + \sum_{j=N_k}^{N-1} F(\Phi_j) \\ &= \sum_{i=0}^{k-1} \eta_i + \sum_{i=0}^{k-1} \xi_i - \sum_{i=0}^{k-1} \zeta_i + \sum_{j=N_k}^{N-1} F(\Phi_j), \\ &= \Xi_k^{(1)} + \Xi_k^{(2)} + \Xi_k^{(3)} + \Xi_{k,N}^{(4)}. \end{aligned} \quad (\text{B.8})$$

Since our estimator of interest is $\hat{f}_n^\Phi = \frac{1}{n} S_n$, it only remains to study the asymptotic behaviour of $\Xi_k^{(m)}$, $m \in \{1, 2, 3\}$, and $\Xi_{k,N}^{(4)}$ as N becomes large and the adaptive parameter γ_i varies.

We follow the steps of the proofs found in Chimisov, Łatuszyński, and Roberts 2018, Section 7. Our scenario has the advantage that, since our original minorisation condition (4.1) was uniform over the sample space, our ergodic atom has geometric return times. However, we have the difficulty that our (Φ, Y) regenerations are 2-step regenerations, rather than 1-step regenerations, which means that our excursions are 1-dependent, not independent.

We write expectations of the form $\mathbb{E}_{(\phi,y)}^{\gamma_0}$ as expectations with initial value (ϕ, y) and initial adaptive parameter γ_0 . If integrands are independent of the initial values (Φ_0, Y_0) , we shall simply write \mathbb{E}^γ . The underlying adaptation scheme which updates γ_k is then assumed to be included in the relevant expectations.

B.1 Asymptotic Behaviour of $\Xi_k^{(2)}$

Since most of the sample path will be contained in the $\Xi_k^{(2)}$ term, we start by studying its properties. The other terms can be controlled relatively easily thanks

to the boundedness of f and the geometric tails of distribution of the excursion lengths.

We define the asymptotic variance function as:

$$\sigma^2(\gamma) = \epsilon \mathbb{E}^\gamma(\xi_{1,1}^2) + 2\epsilon \mathbb{E}^\gamma(\xi_{1,1}\xi_{1,2}) \quad (\text{B.9})$$

not to be confused with the stopping times $\sigma_j^{(i)}$. We have that:

$$\begin{aligned} \mathbb{E}^\gamma(\xi_{1,1}^2) &= \mathbb{E}^\gamma\left(\left[\sum_{m=\check{T}_1+1}^{\check{T}_2} F(\Phi_m)\right]^2\right) = \mathbb{E}^\gamma\left(\left[\sum_{m=\check{\tau}_1+2}^{\check{\tau}_2+1} F(\Phi_m)\right]^2\right) \\ &= \mathbb{E}_{\nu^*}^\gamma\left(\left[\sum_{m=1}^{\check{\sigma}_1+1} F(\Phi_m)\right]^2\right), \end{aligned} \quad (\text{B.10})$$

so since f is bounded and $\check{\sigma}_1 \sim \text{Geom}(\epsilon)$, we can use the Cauchy-Schwartz inequality to get:

$$\sup_{\gamma \in \Gamma} \sigma^2(\gamma) < \infty. \quad (\text{B.11})$$

We start by giving explicit expressions for the moments of ξ_i :

Lemma B.1 (Moments of ξ_i). *Consider $\xi_{i,j}$ and ξ_i as given in Equation (B.6). Then, if $\mathbb{E}_{\pi_\gamma}(f(X)) = 0$:*

$$\begin{aligned} \mathbb{E}^{\gamma_0}(\xi_{i,j}|\gamma_i) &= \mathbb{E}^{\gamma_0}(\xi_i|\gamma_i) = 0, \\ \mathbb{E}^{\gamma_0}(\xi_i^2|\gamma_i) &= (n_{i+1} - 1)\sigma^2(\gamma_i) - 2\mathbb{E}^{\gamma_i}(\xi_{1,1}\xi_{1,2}), \\ \mathbb{E}^{\gamma_0}(\xi_i^4|\gamma_i) &= \mathcal{O}(n_{i+1}^2), \end{aligned}$$

where the \mathcal{L}^4 bound holds uniformly over γ_i .

The first statement follows from standard relations between excursions and stationary measures. The second statement follows from Wald's identity. The third statement follows from a martingale argument using Doob's inequality.

Proof of Lemma B.1. For $i \geq 0$ fixed, recall that $\xi_{i,j}$ are identically distributed random variables. We therefore have that:

$$\begin{aligned} \mathbb{E}^{\gamma_0}(\xi_{i,j}|\gamma_i) &= \mathbb{E}^{\gamma_0}\left(\sum_{m=T_j^{(i)}+1}^{T_{j+1}^{(i)}} F(H_m^{(i)}) \middle| \gamma_i\right) \\ &= \mathbb{E}^{\gamma_i}\left(\sum_{m=\check{T}_j+1}^{\check{T}_{j+1}} F(\Phi_m)\right), \end{aligned}$$

must be constant over j . By Theorem 10.0.1 of Meyn and Tweedie 2012, we have that:

$$\mathbb{E}_{\check{\pi}_\gamma}^\gamma \left(\mathbb{1}(Y_0 = 1) \sum_{m=1}^{\check{\tau}_1} F(\Phi_m) \right) = \mathbb{E}_{\check{\pi}_\gamma}(F(\Phi)) = 0.$$

Writing $\check{\pi}|_{\check{\alpha}}(\cdot) = \epsilon^{-1} \check{\pi}_\gamma(\cdot \cap \{Y = 1\})$, we rewrite this as:

$$\mathbb{E}_{\check{\pi}|_{\check{\alpha}}}^\gamma \left(\sum_{m=1}^{\check{\tau}_1} F(\Phi_m) \right) = \epsilon^{-1} \mathbb{E}_{\check{\pi}_\gamma}^\gamma \left(\mathbb{1}(Y_0 = 1) \sum_{m=1}^{\check{\tau}_1} F(\Phi_m) \right) = 0. \quad (\text{B.12})$$

Exactly as in Equation (B.10), for any initial distribution μ :

$$\mathbb{E}_\mu^\gamma \left(\sum_{m=\check{T}_j+1}^{\check{T}_{j+1}} F(\Phi_m) \right) = \mathbb{E}_{\nu^*}^\gamma \left(\sum_{m=1}^{\check{\sigma}_1+1} F(\Phi_m) \right).$$

Comparing this with Equation (B.12), we see that:

$$\begin{aligned} \mathbb{E}_{\nu^*}^\gamma \left(\sum_{m=1}^{\check{\sigma}_1+1} F(\Phi_m) \right) &= \mathbb{E}_{\check{\pi}|_{\check{\alpha}}}^\gamma \left(\sum_{m=\check{\sigma}_1+2}^{\check{\sigma}_2+1} F(\Phi_m) \right) \\ &= \mathbb{E}_{\check{\pi}|_{\check{\alpha}}}^\gamma \left(\sum_{m=1}^{\check{\tau}_1} F(\Phi_m) \right) + \mathbb{E}_{\check{\pi}|_{\check{\alpha}}}^\gamma (F(\Phi_{\check{\sigma}_2+1})) - \mathbb{E}_{\check{\pi}|_{\check{\alpha}}}^\gamma (F(\Phi_1)) \\ &= \mathbb{E}_{\check{\pi}|_{\check{\alpha}}}^\gamma (F(\Phi_{\check{T}_2})) - \mathbb{E}_{\check{\pi}|_{\check{\alpha}}}^\gamma (F(\Phi_1)). \end{aligned}$$

However, Lemma A.2 tells us that, given $\Phi_0(T) \sim \pi_\gamma$ and $Y_0 = 1$, we have that Φ_1 and $\Phi_{\check{T}_2}$ have the same distribution. Hence:

$$\mathbb{E}_{\nu^*}^\gamma \left(\sum_{m=1}^{\check{\sigma}_1+1} F(\Phi_m) \right) = 0 \quad \implies \quad \mathbb{E}^{\gamma_0}(\xi_{i,j}|\gamma_i) = 0. \quad (\text{B.13})$$

For $\mathbb{E}^{\gamma_0}(\xi_i|\gamma_i) = \mathbb{E}^{\gamma_0}(\sum_{j=1}^{L_i-1} \xi_{i,j}|\gamma_i)$, we use Wald's identity. For this, we require that:

$$\mathbb{E}^{\gamma_0}(\xi_{i,j} \mathbb{1}(L_i - 1 \geq j)|\gamma_i) = \mathbb{E}^{\gamma_0}(\xi_{i,j}|\gamma_i) \mathbb{P}^{\gamma_0}(L_i - 1 \geq j), \quad (\text{B.14})$$

for every j (recalling that $\sigma_j^{(i)}$ are independent of γ_i , so L_i is also).

However, $\{L_i - 1 \geq j\} = \{T_j^{(i)} < n_{i+1} - 1\} = \{\sigma_j^{(i)} \leq n_{i+1} - 3\}$. Since $\xi_{i,j}$ is a function of the excursion $\Psi_j^{(i)}$, it is independent of the event $\{\sigma_j^{(i)} \leq n_{i+1} - 3\}$, giving the required condition.

Thus, we can apply Wald's identity to get that:

$$\mathbb{E}^{\gamma_0}(\xi_i|\gamma_i) = \mathbb{E}^{\gamma_0}\left(\sum_{j=1}^{L_i-1} \xi_{i,j} \middle| \gamma_i\right) = \mathbb{E}^{\gamma_0}(L_i - 1) \times \mathbb{E}^{\gamma_0}(\xi_{i,1}|\gamma_i) = 0. \quad (\text{B.15})$$

For $\mathbb{E}^{\gamma_0}(\xi_i^2|\gamma_i)$, we follow an argument similar to the standard proof of Wald's identity:

$$\begin{aligned} \mathbb{E}^{\gamma_0}(\xi_i^2|\gamma_i) &= \mathbb{E}^{\gamma_0}\left(\left[\sum_{j=1}^{L_i-1} \xi_{i,j}\right]^2 \middle| \gamma_i\right) \\ &= \mathbb{E}^{\gamma_0}\left(\left[\sum_{j=1}^{\infty} \xi_{i,j} \mathbb{1}(\sigma_j^{(i)} \leq n_{i+1} - 3)\right]^2 \middle| \gamma_i\right) \\ &= \sum_{j=1}^{\infty} \mathbb{E}^{\gamma_0}\left(\xi_{i,j}^2 \mathbb{1}(\sigma_j^{(i)} \leq n_{i+1} - 3) \middle| \gamma_i\right) \\ &\quad + 2 \sum_{j < k} \mathbb{E}^{\gamma_0}\left(\xi_{i,j} \xi_{i,k} \mathbb{1}(\sigma_j^{(i)} \leq n_{i+1} - 3) \mathbb{1}(\sigma_k^{(i)} \leq n_{i+1} - 3) \middle| \gamma_i\right) \\ &= \sum_{j=1}^{\infty} \mathbb{E}^{\gamma_0}\left(\xi_{i,j}^2 \mathbb{1}(\sigma_j^{(i)} \leq n_{i+1} - 3) \middle| \gamma_i\right) \\ &\quad + 2 \sum_{j < k} \mathbb{E}^{\gamma_0}\left(\xi_{i,j} \xi_{i,k} \mathbb{1}(\sigma_k^{(i)} \leq n_{i+1} - 3) \middle| \gamma_i\right), \end{aligned}$$

since $j < k \implies \sigma_j^{(i)} < \sigma_k^{(i)}$. The first sum, using Wald's identity, can be simplified to:

$$\sum_{j=1}^{\infty} \mathbb{E}^{\gamma_0}\left(\xi_{i,j}^2 \mathbb{1}(\sigma_j^{(i)} \leq n_{i+1} - 3) \middle| \gamma_i\right) = \mathbb{E}^{\gamma_0}(L_i - 1) \times \mathbb{E}^{\gamma_0}(\xi_{i,1}^2|\gamma_i). \quad (\text{B.16})$$

For the second term, if we condition on the σ -algebra $\mathcal{F}_{T_{j+1}^{(i)}}$ and $k > j + 1$, then the 1-dependent structure of the excursions gives that $\xi_{i,k}$ is conditionally independent of $\xi_{i,j} \mathbb{1}(\sigma_k^{(i)} \leq n_{i+1} - 3)$ and these expectations must be 0. Thus:

$$\sum_{j < k} \mathbb{E}^{\gamma_0}\left(\xi_{i,j} \xi_{i,k} \mathbb{1}(\sigma_k^{(i)} \leq n_{i+1} - 3) \middle| \gamma_i\right) = \sum_{j=1}^{\infty} \mathbb{E}^{\gamma_0}\left(\xi_{i,j} \xi_{i,j+1} \mathbb{1}(\sigma_{j+1}^{(i)} \leq n_{i+1} - 3) \middle| \gamma_i\right). \quad (\text{B.17})$$

Since $\xi_{i,j+1}$ is independent of $\{H_m^{(i)}\}_{m=0}^{\sigma_{j+1}^{(i)}}$ conditionally on γ_i , we have that:

$$\mathbb{E}^{\gamma_0}\left(\xi_{i,j} \xi_{i,j+1} \mathbb{1}(\sigma_{j+1}^{(i)} \leq n_{i+1} - 3) \middle| \gamma_i\right)$$

$$\begin{aligned}
&= \mathbb{E}^{\gamma_0} \left(F(\Phi_{T_{j+1}^{(i)}}) \xi_{i,j+1} \mathbb{1}(\sigma_{j+1}^{(i)} \leq n_{i+1} - 3) \middle| \gamma_i \right) \\
&\quad + \mathbb{E}^{\gamma_0}(\xi_{i,j+1} | \gamma_i) \mathbb{E}^{\gamma_0} \left(\mathbb{1}(\sigma_{j+1}^{(i)} \leq n_{i+1} - 3) [\xi_{i,j} - F(\Phi_{T_{j+1}^{(i)}})] \middle| \gamma_i \right) \\
&= \mathbb{E}^{\gamma_0} \left(F(\Phi_{T_{j+1}^{(i)}}) \xi_{i,j+1} \mathbb{1}(\sigma_{j+1}^{(i)} \leq n_{i+1} - 3) \middle| \gamma_i \right).
\end{aligned}$$

However, if we condition on the σ -algebra $\mathcal{F}_{\sigma_{j+1}^{(i)}}^Y$, the σ -algebra generated by the Y components of the sequence $H_m^{(i)}$ up to the stopping time $\sigma_{j+1}^{(i)}$, then from Lemma A.2 we know that the distribution of $\Phi_{T_{j+1}^{(i)}}$ is a bridge segment starting according to π_γ and ending according to ν . This conditional expectation is therefore constant over j . Thus, we can write:

$$\begin{aligned}
\mathbb{E}^{\gamma_0} \left(\xi_{i,j} \xi_{i,j+1} \mathbb{1}(\sigma_{j+1}^{(i)} \leq n_{i+1} - 3) \middle| \gamma_i \right) &= \mathbb{E}^{\gamma_0} \left(F(\Phi_{T_{j+1}^{(i)}}) \xi_{i,j+1} \middle| \gamma_i \right) \\
&\quad \times \mathbb{P}^{\gamma_0}(\sigma_{j+1}^{(i)} \leq n_{i+1} - 3) \\
&= \mathbb{E}^{\gamma_0} \left(\xi_{i,j} \xi_{i,j+1} \middle| \gamma_i \right) \mathbb{P}^{\gamma_0}(L_i - 1 \geq j + 1),
\end{aligned}$$

since $\xi_{i,j+1}$ is conditionally independent of $\{H_m^{(i)}\}_{m=0}^{\sigma_{j+1}^{(i)}}$.

Thus, we get that:

$$\sum_{j=1}^{\infty} \mathbb{E}^{\gamma_0} \left(\xi_{i,j} \xi_{i,j+1} \mathbb{1}(\sigma_{j+1}^{(i)} \leq n_{i+1} - 3) \middle| \gamma_i \right) = \mathbb{E}^{\gamma_0}(\xi_{i,1} \xi_{i,2} | \gamma_i) \mathbb{E}^{\gamma_0}(L_i - 2). \quad (\text{B.18})$$

Combining Equations (B.16) and (B.18) gives:

$$\begin{aligned}
\mathbb{E}^{\gamma_0}(\xi_i^2 | \gamma_i) &= \mathbb{E}^{\gamma_0}(\xi_{i,1}^2 | \gamma_i) \times \mathbb{E}^{\gamma_0}(L_i - 1) \\
&\quad + 2\mathbb{E}^{\gamma_0}(\xi_{i,1} \xi_{i,2} | \gamma_i) \times \mathbb{E}^{\gamma_0}(L_i - 2).
\end{aligned} \quad (\text{B.19})$$

For $\mathbb{E}^{\gamma_0}(L_i)$, we have that:

$$\mathbb{E}^{\gamma_0}(L_i) = 1 + \sum_{j=0}^{n_{i+1}-2} \mathbb{P}^{\gamma_0}(H_j^{(i)} \in \check{\alpha}) = 1 + \epsilon(n_{i+1} - 1), \quad (\text{B.20})$$

for $i \geq 2$. The fixed value of $Y_0 = y$ will slightly skew the expectation of L_1 , but this is asymptotically irrelevant, or can be removed by taking $Y_0 \sim \text{Bern}(\epsilon)$.

We therefore get that:

$$\begin{aligned}
\mathbb{E}^{\gamma_0}(\xi_i^2 | \gamma_i) &= \epsilon(n_{i+1} - 1) \mathbb{E}^{\gamma_0}(\xi_{i,1}^2 | \gamma_i) \\
&\quad + 2[\epsilon(n_{i+1} - 1) - 1] \mathbb{E}^{\gamma_0}(\xi_{i,1} \xi_{i,2} | \gamma_i) \\
&= (n_{i+1} - 1) \sigma^2(\gamma_i) - 2\mathbb{E}^{\gamma_i}(\xi_{1,1} \xi_{1,2}).
\end{aligned} \quad (\text{B.21})$$

This leaves $\mathbb{E}^{\gamma_0}(\xi_i^4|\gamma_i)$, for which we rely on a crude upper bound using Doob's L_p inequality. We have that:

$$\begin{aligned}\mathbb{E}^{\gamma_0}(\xi_i^4|\gamma_i) &= \mathbb{E}^{\gamma_0}\left(\left[\sum_{j=1}^{L_i-1}\xi_{i,j}\right]^4\middle|\gamma_i\right) \\ &\leq \mathbb{E}^{\gamma_0}\left(\max_{m=0,\dots,n_{i+1}-1}\left[\sum_{j=1}^m\xi_{i,j}\right]^4\middle|\gamma_i\right).\end{aligned}\tag{B.22}$$

Since $\xi_{i,j}$ are conditionally 1-dependent, $\{\sum_{j=1}^m\xi_{i,j}\}_{m\geq 0}$ is not a martingale, even conditionally on γ_i . As in Bednorz, Łatuszyński, and Latała 2008, Section 4, we can divide this sum into odd and even terms since:

$$\left[\sum_{j=1}^m\xi_{i,j}\right]^4 \leq 2^3\left(\left[\sum_{\substack{j=1 \\ j \text{ odd}}}^m\xi_{i,j}\right]^4 + \left[\sum_{\substack{j=1 \\ j \text{ even}}}^m\xi_{i,j}\right]^4\right),\tag{B.23}$$

by Jensen's inequality. These two sums are martingales because, conditionally on γ_i , $\{\xi_{i,2j}\}_{j\geq 1}$ and $\{\xi_{i,2j-1}\}_{j\geq 1}$ are iid sequences of mean 0 random variables. So we get that:

$$\begin{aligned}\mathbb{E}^{\gamma_0}(\xi_i^4|\gamma_i) &\leq 8\mathbb{E}^{\gamma_0}\left(\max_{m=0,\dots,n_{i+1}-1}\left[\sum_{\substack{j=1 \\ j \text{ odd}}}^m\xi_{i,j}\right]^4\middle|\gamma_i\right) \\ &\quad + 8\mathbb{E}^{\gamma_0}\left(\max_{m=0,\dots,n_{i+1}-1}\left[\sum_{\substack{j=1 \\ j \text{ even}}}^m\xi_{i,j}\right]^4\middle|\gamma_i\right) \\ &\leq 8\left(\frac{4}{3}\right)^4 \times \mathbb{E}^{\gamma_0}\left(\left[\sum_{\substack{j=1 \\ j \text{ odd}}}^{n_{i+1}-1}\xi_{i,j}\right]^4 + \left[\sum_{\substack{j=1 \\ j \text{ even}}}^{n_{i+1}-1}\xi_{i,j}\right]^4\middle|\gamma_i\right),\end{aligned}\tag{B.24}$$

by Doob's L_p inequality.

By conditional independence, we have that:

$$\begin{aligned}\mathbb{E}^{\gamma_0}\left(\left[\sum_{\substack{j=1 \\ j \text{ odd}}}^{n_{i+1}-1}\xi_{i,j}\right]^4\middle|\gamma_i\right) &= \left\lceil\frac{n_{i+1}-1}{2}\right\rceil\mathbb{E}^{\gamma_i}(\xi_{1,1}^4) \\ &\quad + \left\lceil\frac{n_{i+1}-1}{2}\right\rceil\left(\left\lceil\frac{n_{i+1}-1}{2}\right\rceil - 1\right)\mathbb{E}^{\gamma_i}(\xi_{1,1}^2)^2, \\ \mathbb{E}^{\gamma_0}\left(\left[\sum_{\substack{j=1 \\ j \text{ even}}}^{n_{i+1}-1}\xi_{i,j}\right]^4\middle|\gamma_i\right) &= \left\lfloor\frac{n_{i+1}-1}{2}\right\rfloor\mathbb{E}^{\gamma_i}(\xi_{1,1}^4)\end{aligned}$$

$$+ \left\lfloor \frac{n_{i+1} - 1}{2} \right\rfloor \left(\left\lfloor \frac{n_{i+1} - 1}{2} \right\rfloor - 1 \right) \mathbb{E}^{\gamma_i}(\xi_{1,1}^2)^2.$$

Substituting these into Equation (B.24) simplifies to give:

$$\begin{aligned} \mathbb{E}^{\gamma_0}(\xi_i^4 | \gamma_i) &\leq \frac{2048}{81} \left((n_{i+1} - 1) \mathbb{E}^{\gamma_i}(\xi_{1,1}^4) + \frac{(n_{i+1} - 2)^2}{2} \mathbb{E}^{\gamma_i}(\xi_{1,1}^2)^2 \right) \\ &= \mathcal{O}(n_{i+1}^2), \end{aligned} \quad (\text{B.25})$$

uniformly over γ_i , assuming that $\sup_{\gamma \in \Gamma} \left(\mathbb{E}^{\gamma}(\xi_{1,1}^4) \right) < +\infty$, which follows from the fact that f is bounded and $\check{\sigma}_1 \sim \text{Geom}(\epsilon)$. QED

For the asymptotic results, the vast majority of our process is contained within the $\Xi_k^{(2)}$ terms, so we shall start by considering those.

Lemma B.2 (L_2 Convergence of $\Xi^{(2)}$). *Consider $\Xi_k^{(2)}$ as given in Equation (B.8). Then, assuming $\mathbb{E}_{\pi_\gamma}(f(X)) = 0$ for all $\gamma \in \Gamma$, we have that $\forall (\phi, y) \in \check{\Omega}$ and $\gamma_0 \in \Gamma$:*

$$\mathbb{E}^{\gamma_0}(\Xi_k^{(2)}) = 0,$$

and:

$$\mathbb{E}^{\gamma_0} \left(\left[\frac{1}{N_k} \Xi_k^{(2)} \right]^2 \right) = \mathcal{O} \left(\frac{1}{N_k} \right),$$

as $k \rightarrow +\infty$.

The proof of this Lemma follows relatively easily from Lemma B.1.

Proof of Lemma B.2. The fact that $\mathbb{E}^{\gamma_0}(\Xi_k^{(2)}) = 0$ follows directly from the fact that $\mathbb{E}^{\gamma_0}(\xi_i) = 0$.

For $\mathbb{E}^{\gamma_0} \left(\left[\frac{1}{N_k} \Xi_k^{(2)} \right]^2 \right)$, we start by noting that:

$$\mathbb{E}^{\gamma_0}(\xi_i \xi_j) = 0, \quad (\text{B.26})$$

for every $i \neq j$, which follows from a conditioning argument. Thus:

$$\mathbb{E}^{\gamma_0} \left((\Xi_k^{(2)})^2 \right) = \sum_{i=0}^{k-1} \mathbb{E}^{\gamma_0}(\xi_i^2). \quad (\text{B.27})$$

Since $\sigma^2(\gamma)$ and $\mathbb{E}^{\gamma}(\xi_{1,1}^2)$ are bounded uniformly over $\gamma \in \Gamma$, we have that:

$$\begin{aligned} \mathbb{E}^{\gamma_0}(\xi_i^2) &\leq (n_{i+1} - 1) \mathbb{E}^{\gamma_0}(\sigma^2(\gamma_i)) + 2 \left| \mathbb{E}^{\gamma_0}(\xi_{i,1} \xi_{i,2}) \right| \\ &\leq (n_{i+1} - 1) \sup_{\gamma \in \Gamma} (\sigma^2(\gamma)) + 2 \sup_{\gamma \in \Gamma} (\mathbb{E}^{\gamma}(\xi_{1,1}^2)). \end{aligned} \quad (\text{B.28})$$

By Equation (B.27), this gives:

$$\begin{aligned} \mathbb{E}^{\gamma_0} \left((\Xi_k^{(2)})^2 \right) &= \sum_{i=0}^{k-1} \mathbb{E}^{\gamma_0} (\xi_i^2) \leq (N_k - k) \sup_{\gamma \in \Gamma} (\sigma^2(\gamma)) \\ &\quad + 2k \sup_{\gamma \in \Gamma} (\mathbb{E}^\gamma (\xi_{1,1}^2)), \end{aligned} \quad (\text{B.29})$$

so:

$$\begin{aligned} \mathbb{E}^{\gamma_0} \left(\left(\frac{1}{N_k} \Xi_k^{(2)} \right)^2 \right) &\leq \sup_{\gamma \in \Gamma} (\sigma^2(\gamma)) \left[\frac{k}{N_k^2} + \frac{1}{N_k} \right] \\ &\quad + \frac{2k}{N_k^2} \sup_{\gamma \in \Gamma} (\mathbb{E}^\gamma (\xi_{1,1}^2)) \\ &= \mathcal{O} \left(\frac{1}{N_k} \right), \end{aligned} \quad (\text{B.30})$$

as required, since $N_k \geq k$. QED

With this bound on second moments, we can move onto a CLT for $\Xi_k^{(2)}$.

Lemma B.3 (Central Limit Theorem for $\Xi_k^{(2)}$). *Consider $\Xi_k^{(2)}$ as given in Equation (B.8). Assume $\mathbb{E}_\pi(f(X)) = 0$, and that $\sigma^2(\gamma)$ is a continuous function of γ . Suppose also that $\gamma_i \xrightarrow{P} \gamma_\infty$ as $i \rightarrow +\infty$, where γ_∞ is constant. Then, if $\sigma^2(\gamma_\infty) > 0$, we have that $\forall(\phi, y) \in \tilde{\Omega}, \gamma_0 \in \Gamma$:*

$$\frac{1}{\sqrt{N_k}} \Xi_k^{(2)} \xrightarrow{D} \mathcal{N}(0, \sigma^2(\gamma_\infty))$$

as $k \rightarrow +\infty$.

We will show later, using results following from Lemma B.2 and others, that the assumptions on the convergence of γ_i are not particularly restrictive for well chosen parameter estimators.

We follow a similar proof to the CLT proof for $\Xi_k^{(2)}$ in Chimisov, Łatuszyński, and Roberts 2018, based on Theorem 2.2 from Dvoretzky 1972.

Proof of Lemma B.3. We intend to apply Theorem 2.2 from Dvoretzky 1972 with $X_{n,k} = \frac{1}{\sqrt{N_n \sigma^2(\gamma_n)}} \xi_k$, though our indices do not quite line up with theirs.

Let:

$$\tilde{\mathcal{F}}_{-1} = \sigma(\gamma_0), \quad \tilde{\mathcal{F}}_i = \sigma \left(\tilde{\mathcal{F}}_{i-1} \cup \{\xi_{i,j}\}_{j \geq 1} \cup \{\gamma_{i+1}\} \right), \quad (\text{B.31})$$

for $i \geq 0$. From Lemma B.1, we have $\mathbb{E}^{\gamma_0}(\xi_i | \tilde{\mathcal{F}}_{i-1}) = \mathbb{E}^{\gamma_0}(\xi_i | \gamma_i) = 0$, which gives condition (2.3) from Dvoretzky 1972.

Also by Lemma B.1, we have that:

$$\mathbb{E}^{\gamma_0}(\xi_i^2 | \tilde{\mathcal{F}}_{i-1}) = \mathbb{E}^{\gamma_0}(\xi_i^2 | \gamma_i) = (n_{i+1} - 1)\sigma^2(\gamma_i) - 2\mathbb{E}^{\gamma_i}(\xi_{1,1}\xi_{1,2}). \quad (\text{B.32})$$

This gives that:

$$\sum_{i=0}^{k-1} \mathbb{E}^{\gamma_0}(\xi_i^2 | \tilde{\mathcal{F}}_{i-1}) = \sum_{i=0}^{k-1} (n_{i+1} - 1)\sigma^2(\gamma_i) - 2 \sum_{i=0}^{k-1} \mathbb{E}^{\gamma_i}(\xi_{1,1}\xi_{1,2}). \quad (\text{B.33})$$

Assuming that $\gamma_i \xrightarrow{P} \gamma_\infty$ as $i \rightarrow +\infty$, and assuming that $\sigma^2(\gamma)$ is continuous in γ , we get that $\sigma^2(\gamma_i) \xrightarrow{P} \sigma^2(\gamma_\infty)$ as $i \rightarrow +\infty$. Since $\sigma^2(\gamma)$ is uniformly bounded, it follows also that $\sigma^2(\gamma_i) \xrightarrow{L^1} \sigma^2(\gamma_\infty)$ as $i \rightarrow +\infty$.

From this, it is easy to show that:

$$\frac{1}{N_k} \sum_{i=0}^{k-1} \mathbb{E}^{\gamma_0}(\xi_i^2 | \tilde{\mathcal{F}}_{i-1}) \xrightarrow{L^1} \sigma^2(\gamma_\infty), \quad \text{as } k \rightarrow +\infty, \quad (\text{B.34})$$

which implies condition (2.4) from Dvoretzky 1972.

It remains for us to show the following Lindeberg condition:

$$\frac{1}{N_k} \sum_{i=0}^{k-1} \mathbb{E}^{\gamma_0}(\xi_i^2 \mathbb{1}(\xi_i^2 > \delta N_k) | \tilde{\mathcal{F}}_{i-1}) \xrightarrow{P} 0, \quad (\text{B.35})$$

as $k \rightarrow +\infty$, for every $\delta > 0$.

Now, we can apply the Cauchy-Schwartz inequality and Markov's inequality to get that:

$$\begin{aligned} \mathbb{E}^{\gamma_0}(\xi_i^2 \mathbb{1}(\xi_i^2 > \delta N_k) | \tilde{\mathcal{F}}_{i-1}) &= \mathbb{E}^{\gamma_0}(\xi_i^2 \mathbb{1}(\xi_i^2 > \delta N_k) | \gamma_i) \\ &\leq \mathbb{E}^{\gamma_0}(\xi_i^4 | \gamma_i)^{1/2} \times \mathbb{P}^{\gamma_0}(\xi_i^2 > \delta N_k | \gamma_i)^{1/2} \\ &\leq \mathbb{E}^{\gamma_0}(\xi_i^4 | \gamma_i)^{1/2} \left[\frac{\mathbb{E}^{\gamma_0}(\xi_i^4 | \gamma_i)}{\delta^2 N_k^2} \right]^{1/2} \\ &= \frac{1}{\delta N_k} \mathbb{E}^{\gamma_0}(\xi_i^4 | \gamma_{i-1}). \end{aligned}$$

By Lemma B.1, we get that $\exists M > 0$ such that:

$$\frac{1}{N_k} \sum_{i=0}^{k-1} \mathbb{E}^{\gamma_0}(\xi_i^2 \mathbb{1}(\xi_i^2 > \delta N_k) | \tilde{\mathcal{F}}_{i-1}) \leq \frac{M \sum_{i=0}^{k-1} n_{i+1}^2}{\delta N_k^2}, \quad (\text{B.36})$$

which goes to 0 as $k \rightarrow +\infty$ by Lemma 1 from Chimisov, Łatuszyński, and Roberts 2018.

Thus, by Theorem 2.2 from Dvoretzky 1972, we get that:

$$\frac{1}{\sqrt{N_k \sigma^2(\gamma_k)}} \Xi_k^{(2)} \xrightarrow{D} \mathcal{N}(0, 1), \quad (\text{B.37})$$

which gives the required result since $\sigma^2(\gamma_k) \xrightarrow{P} \sigma^2(\gamma_\infty)$. QED

B.2 Controlling the Other Terms

We now turn to the remaining terms in Equation (B.8).

Lemma B.4 (Moments of $\Xi_k^{(1)}$, $\Xi_k^{(3)}$ and $\Xi_{k,N}^{(4)}$). *Consider $\Xi_k^{(1)}$, $\Xi_k^{(3)}$ and $\Xi_{k,N}^{(4)}$ as given in Equation (B.8). Then, assuming $\mathbb{E}_\pi(f(X)) = 0$ for f bounded, we have that $\forall(\phi, y) \in \check{\Omega}$ and $\gamma_0 \in \Gamma$:*

$$\mathbb{E}_{(\phi, y)}^{\gamma_0}([\Xi_k^{(1)}]^2) = \mathcal{O}(k^2), \quad \mathbb{E}_{(\phi, y)}^{\gamma_0}([\Xi_k^{(3)}]^2) = \mathcal{O}(k^2),$$

and:

$$\mathbb{E}_{(\phi, y)}^{\gamma_0}([\Xi_{k,N}^{(4)}]^2) = \mathcal{O}(n_{k+1}).$$

The proof of this Lemma follows from Jensen's inequality for $\Xi_k^{(1)}$ and $\Xi_k^{(3)}$, and from a regeneration argument for $\Xi_{k,N}^{(4)}$.

Proof of Lemma B.4. By Jensen's inequality, we have that:

$$\begin{aligned} \mathbb{E}_{(\phi, y)}^{\gamma_0}([\Xi_k^{(1)}]^2) &= \mathbb{E}_{(\phi, y)}^{\gamma_0} \left(\left[\sum_{i=0}^{k-1} \eta_i \right]^2 \right) \\ &\leq k \sum_{i=0}^{k-1} \mathbb{E}_{(\phi, y)}^{\gamma_0}(\eta_i^2) \\ &= k \sum_{i=0}^{k-1} \mathbb{E}_{(\phi, y)}^{\gamma_0} \left(\left[\sum_{j=0}^{T_1^{(i)}} F(H_j^{(i)}) \right]^2 \right) \\ &\leq k^2 M^2 \mathbb{E}((\check{T}_1 + 1)^2), \end{aligned} \quad (\text{B.38})$$

where $|f| \leq M$, and since $T_1^{(i)} \sim \text{Geom}(\epsilon)$ for each i .

Since the renewal sequence $\{T_j^{(i)}\}_{j \geq 1}$ has $\text{Geom}(\epsilon)$ increments and is therefore memoryless, an identical argument gives that:

$$\mathbb{E}_{(\phi, y)}^{\gamma_0}([\Xi_k^{(3)}]^2) \leq k^2 M^2 \mathbb{E}((\check{T}_1 + 1)^2). \quad (\text{B.39})$$

Now, for $\mathbb{E}_{(\phi,y)}^{\gamma_0}([\Xi_{k,N}^{(4)}]^2)$, we follow an identical argument to Lemma B.1. Setting:

$$L^{(4)} = L^{(4)}(k, N) = \inf(l \geq 1 : T_l^{(k+1)} \geq N - N_k - 1), \quad (\text{B.40})$$

we write:

$$\begin{aligned} \eta^{(4)} &= \sum_{j=0}^{T_1^{(k+1)}} F(H_j^{(k+1)}), & \xi^{(4)} &= \sum_{j=T_1^{(k+1)}+1}^{T_{L^{(4)}}^{(k+1)}} F(H_j^{(k+1)}) \\ \zeta^{(4)} &= \sum_{j=N-N_k}^{T_{L^{(4)}}^{(k+1)}} F(H_j^{(k+1)}), & \xi_{i,j}^{(4)} &= \sum_{m=T_j^{(k+1)}+1}^{T_{j+1}^{(k+1)}} F(H_m^{(k+1)}). \end{aligned} \quad (\text{B.41})$$

We can therefore divide $\Xi_{k,N}^{(4)}$ as:

$$\Xi_{k,N}^{(4)} = \eta^{(4)} + \xi^{(4)} - \zeta^{(4)}, \quad (\text{B.42})$$

as we did for s_i in Equation (B.7). Now, by an identical argument to Equations (B.38) and (B.39), we get that:

$$\mathbb{E}_{(\phi,y)}^{\gamma_0}([\eta^{(4)}]^2) = \mathcal{O}(1), \quad \mathbb{E}_{(\phi,y)}^{\gamma_0}([\zeta^{(4)}]^2) = \mathcal{O}(1), \quad (\text{B.43})$$

and by an identical argument to Lemma B.1, we get that:

$$\mathbb{E}_{(\phi,y)}^{\gamma_0}([\xi^{(4)}]^2) = \mathcal{O}(N - N_k) \implies \mathbb{E}_{(\phi,y)}^{\gamma_0}([\xi^{(4)}]^2) = \mathcal{O}(n_{k+1}). \quad (\text{B.44})$$

Using these bounds and Equation (B.42) therefore gives:

$$\mathbb{E}_{(\phi,y)}^{\gamma_0}([\Xi_{k,N}^{(4)}]^2) = \mathcal{O}(n_{k+1}), \quad (\text{B.45})$$

which completes the proof. QED

B.3 Gathering all the Terms

We can now conclude by gathering all the terms. This will yield the results given in Theorem 4.5.

Recall first of all that, from Equation (3.3), we are assuming that $n_k = \Theta(k^\beta)$, which implies $N_k = \Theta(k^{\beta+1})$. We can start by gathering our bounds from Lemma B.1 and B.4 to show the following:

Theorem B.5 (Segment Chain LLN). *Consider $(\Phi_n, Y_n)_{n \geq 0}$ the AIR segment chain process, where the original family of transition kernels $\{P_\gamma\}_{\gamma \in \Gamma}$ have invariant distributions π_γ and satisfy the minorisation condition (4.1). Assume that f is bounded and $\mathbb{E}_{\pi_\gamma}(f(X)) = 0$ for all $\gamma \in \Gamma$. Then $\forall (\Phi_0, Y_0) \in \check{\Omega}$, $\gamma_0 \in \Gamma$, and any adaptation scheme:*

- For any $\beta > 0$,

$$\mathbb{E}_{(\Phi_0, Y_0)}^{\gamma_0} \left(\left[\frac{1}{N} S_N \right]^2 \right) = \mathcal{O} \left(N^{-\min \left(1, \frac{2\beta}{1+\beta} \right)} \right),$$

so that a WLLN holds. For $\beta \geq 1$, this bound is $\mathcal{O}(N^{-1})$.

- For $\beta > \frac{1}{2}$, a SLLN holds:

$$\frac{1}{N} S_N \xrightarrow{a.s.} 0.$$

The proof of this theorem is simply a matter of gathering terms from previous results, and is identical to the proof of Theorem 1 from Chimisov, Łatuszyński, and Roberts 2018.

Proof of Theorem B.5. For the L_2 convergence, note that by Lemma B.1 and B.4, we have:

$$\mathbb{E}_{(\Phi_0, Y_0)}^{\gamma_0} \left(\left[\frac{1}{N_k} S_{N_k} \right]^2 \right) = \mathcal{O} \left(\frac{1}{N_k} \right) + \mathcal{O} \left(\frac{k^2}{N_k^2} \right) + \mathcal{O} \left(\frac{n_{k+1}}{N_k^2} \right).$$

Since $\frac{N_k}{N} \rightarrow 1$ as $N \rightarrow +\infty$, and n_k, N_k are of order k^β and $k^{\beta+1}$ respectively, we get that:

$$\mathbb{E}_{(\Phi_0, Y_0)}^{\gamma_0} \left(\left[\frac{1}{N} S_N \right]^2 \right) = \mathcal{O}(N^{-1}) + \mathcal{O} \left(N^{-\frac{2\beta}{\beta+1}} \right),$$

which gives the L_2 convergence, and hence the WLLN result.

For the SLLN, we appeal to the Borel-Cantelli Lemma. By Chebyshev's inequality, we have that $\forall \delta > 0$:

$$\mathbb{P}_{(\Phi_0, Y_0)}^{\gamma_0} \left(\left| \frac{1}{N_k} S_{N_k} \right| > \delta \right) \leq \delta^{-2} \mathbb{E}_{(\Phi_0, Y_0)}^{\gamma_0} \left(\left[\frac{1}{N_k} S_{N_k} \right]^2 \right) = \mathcal{O}(k^{-(\beta+1)}) + \mathcal{O}(k^{-2\beta}).$$

So, if $\beta > \frac{1}{2}$:

$$\sum_{k=0}^{\infty} \mathbb{P}_{(\Phi_0, Y_0)}^{\gamma_0} \left(\left| \frac{1}{N_k} S_{N_k} \right| > \delta \right) < +\infty. \quad (\text{B.46})$$

The Borel-Cantelli lemma tells us that $\limsup_{k \rightarrow +\infty} \left| \frac{1}{N_k} S_{N_k} \right| \leq \delta$ almost surely. Since this holds for every $\delta > 0$, we get that $\frac{1}{N_k} S_{N_k} \xrightarrow{a.s.} 0$ as $k \rightarrow +\infty$.

Since $\frac{1}{N} S_N = \frac{N_k}{N} \frac{1}{N_k} S_{N_k} + \frac{1}{N} \Xi_{k,N}^{(4)}$, it remains only to show that if $\beta > \frac{1}{2}$, then $\frac{1}{N} \Xi_{k,N}^{(4)} \xrightarrow{a.s.} 0$ as $N \rightarrow +\infty$. However, we have that $\forall \delta > 0$, by Chebyshev's inequality and Lemma B.4:

$$\mathbb{P}_{(\Phi_0, Y_0)}^{\gamma_0} \left(\left| \frac{1}{N} \Xi_{k,N}^{(4)} \right| > \delta \right) = \mathcal{O} \left(\frac{n_{k+1}}{N^2} \right) = \mathcal{O} \left(\frac{n_{k+1}}{N_{k+1}^2} \right).$$

When considering $\sum_{N=1}^{\infty} \mathbb{P}_{(\Phi_0, Y_0)}^{\gamma_0} \left(\left| \frac{1}{N} \Xi_{k,N}^{(4)} \right| > \delta \right)$, for each $k \in \mathbb{N}$ there are n_{k+1} terms of order $\frac{n_{k+1}}{N_{k+1}^2}$. Hence, we can find some $M > 0$ such that:

$$\sum_{N=1}^{\infty} \mathbb{P}_{(\Phi_0, Y_0)}^{\gamma_0} \left(\left| \frac{1}{N} \Xi_{k,N}^{(4)} \right| > \delta \right) \leq M \sum_{k=0}^{\infty} \frac{n_k^2}{N_k^2}. \quad (\text{B.47})$$

Since $\frac{n_k^2}{N_k^2} = \mathcal{O}(k^{-2})$, the LHS is finite. The Borel-Cantelli lemma therefore tells us that $\frac{1}{N} \Xi_{k,N}^{(4)} \xrightarrow{\text{a.s.}} 0$ as required, which concludes the proof. QED

Finally, we prove the central limit theorem for S_N .

Theorem B.6 (Central Limit Theorem for AIR SBPS). *Suppose $\beta > 1$. Consider $(\Phi_n, Y_n)_{n \geq 0}$ the AIR segment chain process, where the original family of transition kernels $\{P_\gamma\}_{\gamma \in \Gamma}$ have invariant distributions π_γ and satisfy the minorisation condition (4.1). Assume that f is bounded and $\mathbb{E}_{\pi_\gamma}(f(X)) = 0$ for all $\gamma \in \Gamma$. Then, if $\gamma_i \xrightarrow{P} \gamma_\infty$ such that $\sigma^2(\gamma_\infty) > 0$, and that $\sigma^2(\gamma)$ is a continuous function of γ , then $\forall (\Phi_0, Y_0) \in \check{\Omega}, \gamma_0 \in \Gamma$:*

$$\frac{1}{\sqrt{N}} S_N \xrightarrow{D} \mathcal{N}(0, \sigma^2(\gamma_\infty)).$$

This theorem follows immediately from Lemma B.3's CLT for $\frac{1}{\sqrt{N_k}} \Xi_k^{(2)}$, then using the moment bounds in Lemma B.4 to show that the other terms go to 0 in probability for large N , assuming $\beta > 1$.

References

- Bednorz, Witold, Krzysztof Łatuszyński, and Rafal Latala (2008). *A regeneration proof of the central limit theorem for uniformly ergodic Markov chains*.
- Bierkens, Joris and Andrew Duncan (2017). “Limit theorems for the zig-zag process”. In: *Advances in Applied Probability* 49.3, pp. 791–825.
- Bierkens, Joris, Paul Fearnhead, and Gareth O Roberts (2019). “The zig-zag process and super-efficient sampling for Bayesian analysis of big data”. In: *International conference on machine learning*. PMLR, pp. 908–918.
- Bierkens, Joris, Sebastiano Grazi, et al. (2020). “The boomerang sampler”. In: *International conference on machine learning*. PMLR, pp. 908–918.
- Bierkens, Joris, Kengo Kamatani, and Gareth O Roberts (2022). “High-dimensional scaling limits of piecewise deterministic sampling algorithms”. In: *The Annals of Applied Probability* 32.5, pp. 3361–3407.

- Bouchard-Côté, Alexandre, Sebastian J Vollmer, and Arnaud Doucet (2018). “The bouncy particle sampler: A nonreversible rejection-free Markov chain Monte Carlo method”. In: *Journal of the American Statistical Association* 113.522, pp. 855–867.
- Chimisov, Cyril, Krzysztof Łatuszyński, and Gareth O Roberts (2018). “Air Markov chain Monte Carlo”. In: *arXiv preprint arXiv:1801.09309*.
- Corbella, Alice, Simon EF Spencer, and Gareth O Roberts (2022). “Automatic Zig-Zag sampling in practice”. In: *Statistics and Computing* 32.6, p. 107.
- Deligiannidis, George, Alexandre Bouchard-Côté, and Arnaud Doucet (2019). “Exponential ergodicity of the bouncy particle sampler”. In.
- Dvoretzky, Aryeh (1972). “Asymptotic normality for sums of dependent random variables”. In: *Proceedings of the Sixth Berkeley Symposium on Mathematical Statistics and Probability, Volume 2: Probability Theory*. Vol. 6. University of California Press, pp. 513–536.
- Gelman, Andrew, Walter R Gilks, and Gareth O Roberts (1997). “Weak convergence and optimal scaling of random walk Metropolis algorithms”. In: *The annals of applied probability* 7.1, pp. 110–120.
- Girolami, Mark and Ben Calderhead (2011). “Riemann manifold langevin and hamiltonian monte carlo methods”. In: *Journal of the Royal Statistical Society Series B: Statistical Methodology* 73.2, pp. 123–214.
- Habeck, Michael et al. (2023). “Geodesic slice sampling on the sphere”. In: *arXiv preprint arXiv:2301.08056*.
- Hastings, W Keith (1970). “Monte Carlo sampling methods using Markov chains and their applications”. In.
- Mengersen, Kerrie L and Richard L Tweedie (1996). “Rates of convergence of the Hastings and Metropolis algorithms”. In: *The annals of Statistics* 24.1, pp. 101–121.
- Metropolis, Nicholas et al. (1953). “Equation of state calculations by fast computing machines”. In: *The journal of chemical physics* 21.6, pp. 1087–1092.
- Meyn, Sean P and Richard L Tweedie (2012). *Markov chains and stochastic stability*. Springer Science & Business Media.
- Neal, Radford M (2012). “MCMC using Hamiltonian dynamics”. In: *arXiv preprint arXiv:1206.1901*.
- Pompe, Emilia, Chris Holmes, and Krzysztof Łatuszyński (2020). “A framework for adaptive MCMC targeting multimodal distributions”. In.
- Roberts, Gareth O and Jeffrey S Rosenthal (2007). “Coupling and ergodicity of adaptive Markov chain Monte Carlo algorithms”. In: *Journal of applied probability* 44.2, pp. 458–475.
- (2009). “Examples of adaptive MCMC”. In: *Journal of computational and graphical statistics* 18.2, pp. 349–367.

- Tawn, Nicholas G, Matthew T Moores, and Gareth O Roberts (2021). “Annealed Leap-Point Sampler for multimodal target distributions”. In: *arXiv preprint arXiv:2112.12908*.
- Vasdekis, Giorgos and Gareth O Roberts (2023). “Speed up zig-zag”. In: *The Annals of Applied Probability* 33.6A, pp. 4693–4746.
- Yang, Jun, Krzysztof Łatuszyński, and Gareth O Roberts (2022). “Stereographic Markov Chain Monte Carlo”. In: *arXiv preprint arXiv:2205.12112*.